NTNU
Norwegian University of
Science and Technology

Lift-off of methane jet flames in O2/CO2 atmospheres

Bård Lode Norheim

Master of Science in Product Design and Manufacturing
Submission date: June 2009
Supervisor: Marie Bysveen, EPT
Co-supervisor: Mario Ditaranto, SINTEF

Norwegian University of Science and Technology
Department of Energy and Process Engineering

Problem Description

The objective is to characterize the stability of methane jet flames in developing in different oxy-fuel atmospheres of varying O2/CO2 concentration, and to compare to a reference case in air. Stability will be evaluated by following the lift-off behavior with different nozzle dimensions. The variation in stoichiometric mixture fraction also influences the flame length. Lift off heights and length will be measured by filtered imaging of the OH* chemiluminecsence at 306 nm, which will also give information on the flame position and its fluctuations. Another aspect of the study is to measure the NOx and CO emissions indices when the fuel is composed of methane and 2 % N2 (synthetic natural gas).

Assignment given: 20. January 2009
Supervisor: Marie Bysveen, EPT

Norwegian University
of Science and Technology
NTNU

Department of Energy
and Process Engineering

EPT-M-2009-

MASTER THESIS

for

Stud.techn.
Spring 2009

Lift-off of methane jet flames in O2/CO2 atmospheres

Lift-off høyde og utslipp av metan flammer i O2/CO2 atmosfærer

Background and objective.

Oxy-fuel combustion is a promising technology to produce power in combination to CO2 capture. However, there is a lack of knowledge on this challenging type of combustion for designing adequately burners, combustors and boilers. Previous studies on the radiative properties of oxy-fuel flames showed major differences as compared to air supported combustion, and further work is required. This study is within the framework of the project BIGCO2, coordinated by SINTEF Energy Research and funded by StatoilHydro, GE Global Research, Statkraft, Aker Kværner, Shell, TOTAL, ConocoPhillips, ALSTOM, the Research Council of Norway (178004/I30 and 176059/I30) and Gassnova (182070).

The objective is to characterize the stability of methane jet flames in developing in different oxy-fuel atmospheres of varying O2/CO2 concentration, and to compare to a reference case in air. Stability will be evaluated by following the lift-off behavior with different nozzle dimensions. The variation in stoichiometric mixture fraction also influences the flame length. Lift off heights and length will be measured by filtered imaging of the OH* chemiluminecsence at 306 nm, which will also give information on the flame position and its fluctuations. Another aspect of the study is to measure the NO_x and CO emissions indices when the fuel is composed of methane and 2 % N_2 (synthetic natural gas).

The following questions should be considered in the project work:

1. What is the lift off (height, blow off and hysteresis) beahvior as a fucntion of Reynolds number when the O2 concetration increases in the CO2 rich atmosphere.
2. What are the mechanisms responsible for NO formation in oxy-fuel flames as a function of O2 concetration in the CO2 rich atmosphere.

I

Within 14 days of receiving the written text on the diploma thesis, the candidate shall submit a research plan for his project to the department.

When the thesis is evaluated, emphasis is put on processing of the results, and that they are presented in tabular and/or graphic form in a clear manner, and that they are analyzed carefully.

The thesis should be formulated as a research report with summary both in English and Norwegian, conclusion, literature references, table of contents etc. During the preparation of the text, the candidate should make an effort to complete a well presented report. In order to ease the evaluation of the thesis, it is important that the cross references are correct. In the making of the report, strong emphasis should b e placed on both a thorough discussion of the results and an orderly presentation.
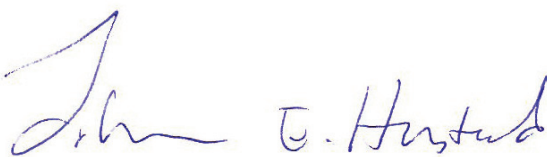
The candidate is requested to initiate and keep close contact with his/her specialist teacher and academic supervisor(s) throughout the working period. The candidate must follow the rules and regulations of NTNU as well as passive directions given by the Department of Energy and Process Engineering.

Pursuant to "Regulations concerning the supplementary provisions to the technology study program/Master of Science" at NTNU §20, the Department reserves the permission to utilize all the results for teaching and research purposes as well as in future publications.
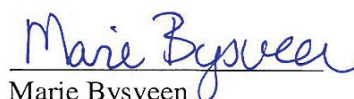
<u>One – 1</u> complete original of the thesis shall be submitted to the authority that handed out the set subject. (A short summary including the author's name and the title of the thesis should also be submitted, for use as reference in journals (max. 1 page with double spacing)).
Two – 2 – copies of the thesis shall be submitted to the Department. Upon request, additional copies shall be submitted directly to research advisors/companies. A CD-ROM (Word format or corresponding) containing the thesis, and including the short summary, must also be submitted to the Department of Energy and Process Engineering

Department of Energy and Process Engineering, 12. January 2009

_____
Professor Johan E. Hustad
Department Manager

Marie Bysveen
Academic Supervisor

Research Advisors:

Mario Ditaranto – SINTEF Energy Research

PREFACE

In my project work last semester I worked on measurements of the radiative heat flux from oxy-fuel combustion and I found the experimental work to be challenging and rewarding. So when I got the opportunity to expand the experimental work into the field of diffusion flame lift-off in oxy-fuel combustion I gladly accepted.

The objective of my master thesis saw some changes as the work progressed and it was discovered that measurements were far more time consuming than initially planned. During meetings with research advisor Mario Ditaranto it was decided that the measurements on exhaust emissions were to be cancelled for this time. Some complications in lift-off measurements, due to the effect of wall temperature, led to the hysteresis experiments being abandoned as well.

During this semester I have spent many weeks in the laboratory, and I believe that I have learned as much about experimental work as I have about turbulent combustion, oxy-fuel combustion and flame lift-off. I have certainly found oxy-fuel combustion to be an interesting field of technology, and I feel convinced that it will play a major part in CO_2 free power production in the future. As I now start my professional career in the oil industry, I do so with a clean conscience, knowing I played a small part in the work towards cleaner power production and reduced CO_2 emissions.

I would like to thank my research advisor Mario Ditaranto for all his help, with regards to both the experimental and theoretical part. Also big thanks to everybody in the work-shop for helping me out when the rig needed modifications and upgrades and when the ventilation needed re-routing.

Trondheim, 16. juni 2009

Bård Lode Norheim

SUMMARY

Turbulent jet diffusion flames and flame lift-off have been the topic of a great deal of research due to its complexity in combining both turbulent flow and combustion. The mechanisms controlling flame lift-off however, are not yet properly understood and is still an active field of research.

In this report, experimental studies of lift-off characteristics for oxy-fuel combustion with methane have been conducted for oxygen concentrations ranging from 34% to 50%. Three different fuel nozzles were used, with diameters of of 2mm, 4mm and 5mm. In addition to oxy-fuel combustion, experiments were carried out in air, and oxygen enriched air, as a reference case.

The goal has been to observe how oxy-fuel flames differ from regular diffusion flames burning in air with regards to lift-off.

Lift-off heights and velocities were found to be strongly dependent on oxygen concentration, with increasing concentration causing shorter lift-off heights and higher lift-off velocities. It was also discovered that the combustion chamber wall temperature seemed to have a great impact on flame stability. Higher wall temperatures had a stabilizing effect on the flame, probably due to lower heat loss and higher burning velocities.

Results from the air cases were compared to data from other studies, and were found to deviate some, most likely due to the presence of co-flow.

SAMMENDRAG

Turbulente diffusjonsflammer og lift-off har vært et aktivt forskingsfelt i lang tid på grunn av kompleksiteten forbundet med både turbulent strømning og forbrenning. Til tross for iherdig forskning er de kontrollerende mekanismene i forbindelse med lift-off fremdeles ikke fullstendig forstått.

I forbindelse med denne oppgaven har det blitt foretatt eksperimentelle studier av lift-off karakteristikker for oxy-fuel flammer i oksygen konsentrasjoner fra 34% til 50%. Brenseldyser med diameter på 2mm, 4mm og 5mm har blitt brukt til hver enkelt flammekonfigurasjon. I tillegg ble det utført forsøk i luft og oksygenanriket luft som referanse.

Målet med oppgaven har vært å observere og kartlegge hvordan oxy-fuel forbrenning skiller seg fra vanlig forbrenning med luft i forbindelse med lift-off.

Det ble funnet at lift-off høyde og hastighet viste høy avhengighet av oksygenkonsentrasjon. Høyere oksygenkonsentrasjon førte til lavere lift-off høyde og høyere lift-off hastighet. Det ble også observert at temperaturen til brennkammerveggen hadde stor innvirkning på flammestabiliteten. Høye veggtemperaturer hadde tilsynelatende en stabiliserende effekt på flammen, sannsynligvis forårsaket av de termiske strålingsegenskapene til karbondioksidgass.

Resultatene fra forsøk med luft ble sammenlignet med resultater fra andre studier, og viste seg å avvike noe, muligens på grunn av forsøkene ble gjort med co-flow i motsetning til sammenligningsgrunnlaget som ble gjort i stille luft.

CONTENT

FIGURES

VIII

1   INTRODUCTION

The focus on climate and global warming in recent times have developed a need for power production without emission of CO_2. Even though new renewable energy sources are being developed and built, they are a long way from replacing power production from fossil fuels like coal and natural gas. This has led to an increased interest for CO_2 capture and storage from power plants, and three major technologies are being investigated.

- Post-combustion removal of CO_2 from the exhaust gas using chemical absorption by amine solutions.
- Pre-combustion decarbonization where CO_2 is removed from the fuel by reforming.
- Oxy-fuel combustion, burning the fuel in pure oxygen to make the exhaust consist of water vapor and CO_2, making separation easier.
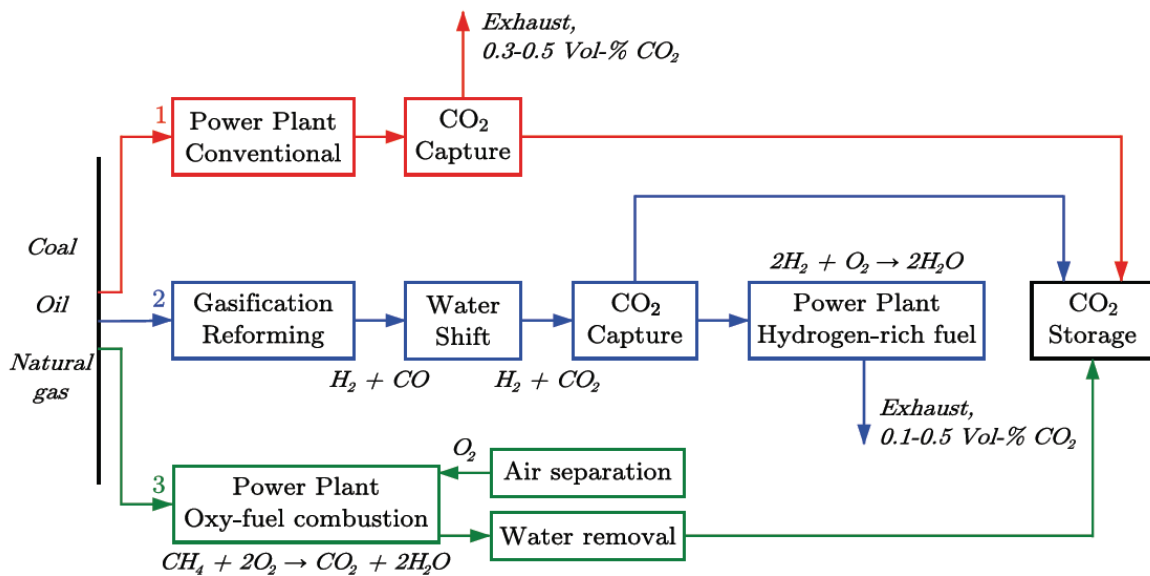
Figure 1 Examples of power production with CO_2 capture

The disadvantage of CO_2 capture and storage is reduced efficiency in power production. Bolland [1] compared the efficiency of power plants with CO_2 capture and storage to a standard combined cycle power plant with 58% efficiency. The results showed that the efficiencies were reduced to 49.6% for pre-combustion capture, 47.2% for oxy-fuel combustion and 45.3% for pre-combustion decarbonization using 90% capture rate.

The focus of this report has been on the combustion process for oxy-fuel flames. Using pure oxygen results in material damaging flame temperatures, therefore it is planned to recycle CO_2 from the flue gas and mix with oxygen. Changing the combustion environment from air to a mixture of oxygen and carbon dioxide alters the combustion properties. Since CO_2 has different properties than nitrogen, various concentrations of O_2 and CO_2 have been used in this report to gain knowledge about the lift-off properties of oxy-fuel combustion.

Lift-off characteristics for non-premixed flames have been, and still is, the subject of numerous research papers. Lyons [2] in 2006 and Pitts [3] in 1998 reviewed the research that had been conducted at the time, and both concluded that the mechanisms involved in lifted turbulent jet flames are not yet fully understood. Lyons concluded that research pointed towards the theories based on premixing and edge flames.

However, no research has been done on the lift-off characteristics of turbulent jet diffusion flames in O_2/CO_2 environment, which is the primary object of this report. In order to achieve a better understanding of this topic, numerous experiments have been conducted in a variety of O_2/CO_2 compositions.

2 BASICS

2.1 COMBUSTION

2.1.1 Reacting mixtures

For complete combustion of methane with air, the reaction is

$$CH_4 + 2(O_2 + 3,76N_2) \rightarrow CO_2 + 2H_2O + 7,52N_2 \tag{2.1}$$
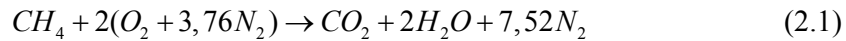
Depending on whether the combustion is fuel rich or fuel lean, there may also be O_2 or CO in the exhaust gas. For the oxy-fuel combustion process, pure oxygen is used instead of air, so the reaction is

$$CH_4 + 2O_2 \rightarrow CO_2 + 2H_2O \tag{2.2}$$

For oxy-fuel combustion in power production, it is planned to recycle CO_2 from the flue gas to dilute the oxygen. CO_2 is mainly inert in the combustion process, so reaction (2.2) will be

$$CH_4 + \frac{2}{\varphi_{O_2}}\left(\varphi_{O_2}O_2 + \varphi_{CO_2}CO_2\right) \rightarrow \left(1 + \frac{2\varphi_{CO_2}}{\varphi_{O_2}}\right)CO_2 + 2H_2O \tag{2.3}$$
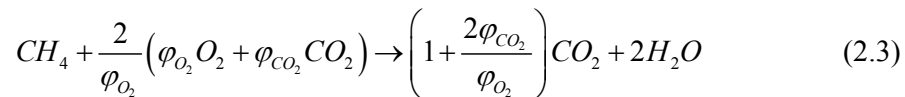
where φ_{O2} and φ_{CO2} are the mol-fractions of oxygen and carbon dioxide in the oxidant gas.

2.1.2 Excess air

AF is the air-to-fuel ratio, and is the ratio of the amount of air in a reaction to the amount of fuel. The ratio can also be written on a molar basis and is then called $\overline{AF}$. The ratio between the actual air-to-fuel ratio and the stochiometric air-to-fuel ratio is expressed $\lambda = \left(\dfrac{AF}{AF_{ST}}\right)$. If $\lambda > 1$ the mixture is fuel-lean and the combustion is complete. For $\lambda < 1$ the mixture is fuel-rich, and unwanted products like CO can be formed in the combustion process. The equivalence ratio $\phi = \lambda^{-1}$ is also used.

2.1.3 Adiabatic Flame Temperature

The adiabatic flame temperature, T_{ad}, is the highest temperature that can be achieved if all energy liberated on combustion is transferred to the combustion products as heat. The adiabatic flame temperature can be determined by use of the conservation of mass and energy principles. Assuming ideal gas principles the energy balance on a mole basis is

$$\sum_P n_e \overline{h_e} = \sum_R n_i \overline{h_i} \tag{2.4}$$

Where e denotes the exiting products, and i the incoming fuel. Using enthalpy of formation the equation takes the form

$$\sum_P n_e \left(\overline{h}_f^0 + \Delta \overline{h} \right)_e = \sum_R n_i \left(\overline{h}_f^0 + \Delta \overline{h} \right)_i \tag{2.5}$$

Using $\Delta \overline{h} = \overline{c}_p \Delta T$ and assuming constant specific heats, the equation becomes

$$\sum_P n_e \left(\overline{c}_p \Delta T \right)_e = \sum_R n_i \left(\Delta \overline{h} \right)_i + \sum_R n_i \left(\overline{h}_f^0 \right)_i - \sum_p n_e \left(\overline{h}_f^0 \right)_e \tag{2.6}$$

Where $\Delta \overline{h}_i = 0$ and the value of c_p is a taken from an assumed $T_{ad.}$, thus solving the equation requires iterations.

2.2 CHEMICAL KINETICS

2.2.1 Global and elementary reactions

The chemical reaction between hydrogen and oxygen to form water is expressed as

$$2H_2 + O_2 \rightarrow 2H_2O \tag{2.7}$$

However, the possibility of exactly two hydrogen molecules colliding with exactly one oxygen molecule, forming two water molecules, all happening instantaneous is unlikely. Reaction (2.7) is actually a simplification, and it is called a global reaction, net reaction, or overall reaction, and is in fact the consequence of several "smaller" reactions called elementary reactions. In the elementary reactions, intermediate species such as O, H and OH are formed. It is apparent that these intermediate species, called radicals or free radicals, are not stable, they are in fact very reactive and quickly form bonds with other molecules. (2.7) is actually a result of more than 20 elementary reactions [4].

$$\begin{aligned} H_2 + O_2 &\rightarrow HO_2 + H \\ H + O_2 &\rightarrow OH + O \\ OH + H_2 &\rightarrow H_2O + H \\ H + O_2 + M &\rightarrow HO_2 + M \end{aligned} \tag{2.8}$$
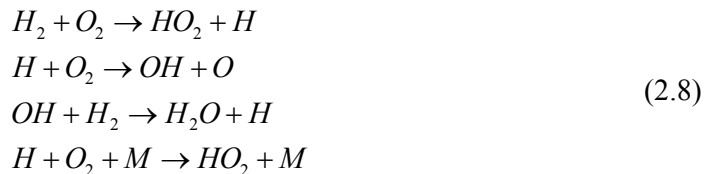
and many others. More complex reactions, such as oxidation of hydrocarbons, may consist of up to several hundred elementary reactions [4].

2.2.2 Reaction Rates

Considering the elementary reaction

$$A + B \rightarrow C + D \tag{2.9}$$

the rate at which A is consumed may be written as

$$\frac{d[A]}{dt} = -k_{bimol}[A][B] \tag{2.10}$$

where k is called the rate coefficient. The value of k is dependent on temperature, and can be calculated from the Arrhenius form

$$k(T) = AT^b \exp(-\frac{E_a}{R_u T}) \tag{2.11}$$

E_a is called the activation energy, and is the energy necessary for the reaction to take place, A is called the pre-exponential factor and R_u is the universal gas constant. Values for A, E_a and b are obtained from experimental data and are found in various tables.

If however, reaction (2.9) above represents not an elementary reaction, but a global one, the rate at which A is consumed is expressed by

$$\frac{d[A]}{dt} = -k_G[A]^a[B]^b \tag{2.12}$$

k_G is called the global rate coefficient. The exponents a and b represent the reaction order, which means that the reaction is of order a with regard to A, b with regard to B, and (a+b) overall. Due to the crudeness in using global reactions, it is difficult to get accurate results from this equation and values for a, b and k_g only hold for small temperature ranges.

2.2.3 Chemical Time Scales

If we consider a unimolecular reaction, $[A] \rightarrow [B]$ we may define $[A]_0$ as the initial concentration of A. The time it takes for the concentration of A to fall from its initial value to a value of *1/e* times that is defined as a chemical time scale, τ_{chem}. For unimolecular reactions it can be found from the apparent rate coefficient as

$$\tau_{chem} = \frac{1}{k_{app}} \tag{2.13}$$

For bimolecular reactions the chemical time scales are also dependent on the initial concentration of the species.

$$\tau_{chem} = \frac{1}{[B]_0 k_{bimolec}} \tag{2.14}$$

The chemical time may also be derived from the flame properties using laminar flame speed and flame thickness.

$$\tau_{chem} = \frac{\delta_l}{S_l} \tag{2.15}$$

The magnitude of chemical time scales spans over a wide range, and may be used as a ratio to convective or mixing times.

2.3   TURBULENCE

Turbulence is " a spatially varying mean flow with superimposed three-dimensional random fluctuations that are self sustaining and enhance mixing, diffusion , entrainment and dissipation." [5]

Figure 2 shows air flowing past a flat plate 2.4m long and 1.2m wide. Transition to turbulence is clearly seen at x ≈ 90cm. The turbulent flow has a much thicker boundary layer as seen in Figure 2b. Smoke is introduced at the beginning of the plate to visualize the shear-layer.
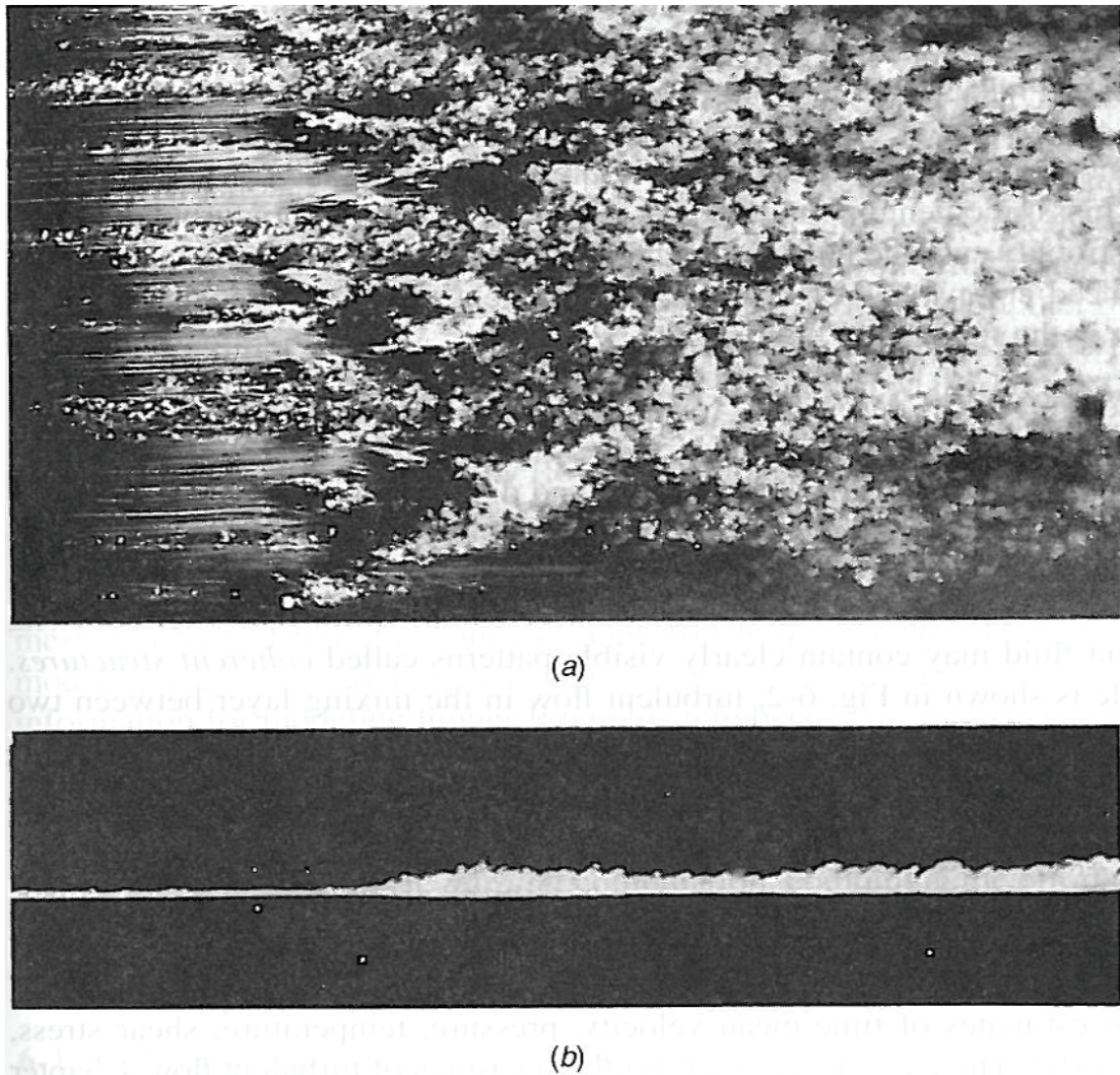
Figure 2 Smoke visualization of airflow at 3.3 m/s past a flat plate: (a) top view (b) side view. Transition is at x ≈ 90cm, or Re ≈ 200000 [5]

The definition above indicates that velocity fluctuates around a mean velocity, in all three dimensions. Fluctuations are caused by eddies, ranging in size from shear layer thickness down to the Kolmogorov length scale. Eddies strongly enhance mixing by moving fluid packets around in the flow, improving diffusion of mass, energy and momentum. The largest eddies get their energy from the mean flow, and are broken down into smaller eddies eventually lost by viscous dissipation. Large eddies are important in mixing the flow, moving fluid packets large distances. In the case of molecular mixing related to combustion however, the smallest eddies vastly improve diffusion compared to laminar flow.

The length scales in turbulent flow ranges from the integral length scale, l_0, based on the dimension of the system, to the Kolmogorov length scale, l_K, which is typically 1/100 of the integral scale[6] describing the size of the smallest turbulent structures. At or below the Kolmogorov length scale, the turbulent kinetic energy is dissipated into heat by viscosity.

Because of the fluctuations in turbulent flow it is normal to split properties into a mean and its fluctuations. The mean flow is defined by

$$\bar{u} = \frac{1}{T} \int_{t_0}^{t_0+T} u \, dt \tag{2.16}$$

and the fluctuation is $u' = u - \bar{u}$. To quantify the magnitude of the fluctuations we use the mean-square value since $\overline{u'} = 0$ by definition

$$\overline{u'^2} = \frac{1}{T} \int_{t_0}^{t_0+T} u'^2 \, dt \tag{2.17}$$

and the root-mean-square is $u'_{rms} = \sqrt{\overline{u'^2}}$. Using the mean and fluctuating values for velocity, temperature and pressure in the basic equations we get the Reynolds equations of turbulent motion.

The degree of turbulence in the flow may be described by the turbulent Reynolds number,

$$R_l = \frac{\bar{\rho}\sqrt{2k}\,l_0}{\bar{\mu}} \tag{2.18}$$

which is defined by the turbulent kinetic energy $k = \frac{1}{2}\overline{u_i u_i}$ and the integral length scale l_0.

There is a relation between the turbulent Reynolds number, the integral length scale and the Kolmogorov length scale

$$R_l = \left(\frac{l_0}{l_K}\right)^{\frac{4}{3}} \tag{2.19}$$

The characteristic flow time or the turbulent timescale is the lifetime of large eddies in the flow, and may defined by

$$\tau_{flow} = \frac{L}{v'} \tag{2.20}$$

The relation between τ_{flow} and τ_{chem} defines an important dimensionless parameter in combustion called the turbulent Damköhler number, from the German combustion scientist Gerhard Damköhler.

$$Da = \frac{\tau_{flow}}{\tau_{chem}} \tag{2.21}$$

There are different Damköhler numbers, and one based on the Kolmogorov time scale, the Karlowitz number, is used in Figure 3. The Karlovitz number (Ka) is another name for the Kolmogorov based Damköhler number Da_K

$$Ka = Da_K = \frac{\tau_K}{\tau_{chem}} \tag{2.22}$$

where τ_K is the Kolmogorov time scale. A diagram representing the various combustion phenomena related to the Damköhler number is shown in Figure 3.
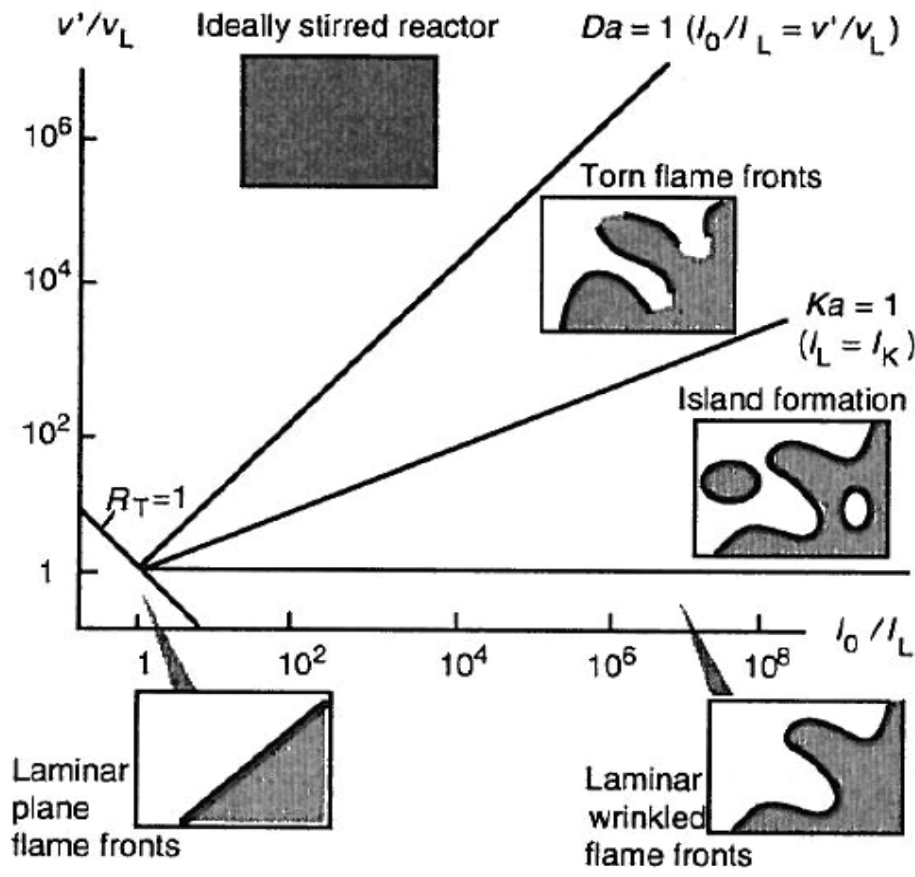
Figure 3 Borghi diagram for flame regimes [6]

Flames with large Da (large τ_{flow}, small τ_{chem}) indicates a thin flat reaction zone, turbulence makes the flame front wrinkled. Increasing turbulence and decreasing Da tears the reaction zone apart and creates "islands" or flamelets. When Da < 1, the time needed for chemical time is greater than the time needed for fluid motion induced change. In this regime, nearly all of the turbulent eddies are embedded in the reaction zone which is so broad that the term "flame front" is not useful [6]. This condition is called an ideally stirred reactor.

2.4   RADIATION

2.4.1   Thermal Radiation

To reach thermal equilibrium, thermal energy is transferred from one surface to another by the propagation of electromagnetic waves or photons, by convection or by conduction. Transfer of thermal energy by the propagation of electromagnetic waves or photons, is called thermal radiation. Thermal radiation has the standard wave properties of wavelength λ and frequency v related by

$$\lambda = \frac{c}{v}$$
(2.23)

where c is the speed of light. In the spectrum of electromagnetic radiation, the portion which spans from about 0.1 μm to about 100 μm, and includes the infrared spectrum, the visible spectrum, and some of the ultraviolet spectrum is called thermal radiation. The magnitude of thermal radiation varies both with respects to the wavelength and its direction. This complicates the calculations, as we have to take into account both the spectral (dependence on wavelength) and the directional (dependence on direction) distribution. A useful quantity in radiation is the spectral intensity, $I_{\lambda,e}$, which is defined as the "rate at which radiant energy is emitted at the wavelength λ in the (θ,φ) direction, per unit area of the emitting surface normal to this direction, per unit solid angle about this direction, and per unit wavelength interval dλ about λ" [7] and is be expressed as

$$I_{\lambda,e}(\lambda,\theta,\varphi) \equiv \frac{dq}{dA_1 \cos\theta \cdot d\omega \cdot d\lambda}$$
(2.24)

If the spectral and directional properties are know, the equation can be rewritten and integrated to give the *total hemispherical emissive power, E* (W/m^2), usually called the *total emissive power*.

$$E = \int_0^\infty \int_0^{2\pi} \int_0^{\frac{\pi}{2}} I_{\lambda,e}(\lambda,\theta,\varphi) \cos\theta \sin\theta d\theta d\varphi d\lambda$$
(2.25)

A often used approximation for the directional distribution is the diffuse emitter, which means a surface where emitted radiation is independent of direction. Using this approximation, and with the spectral distribution known, the total emissive power can be expressed by

$$E = \pi I_e$$
(2.26)

The blackbody is a perfect emitter and absorber, behaving as a diffuse emitter it is used as standard against which actual radiating surfaces may be compared. Using the Planck distribution for spectral intensity, the emissive power of a blackbody is easily calculated using the following equation

$$E_b = \sigma T^4 \tag{2.27}$$

where E_b is the blackbody emissive power, σ is the *Stefan-Boltzman* constant, and T is the absolute temperature (K) of the surface.

2.4.2 Thermal Radiation in Gases

The thermal radiative properties in gases are different from the properties of solids. Air consists mainly of O_2 and N_2 which are nonpolar gases, they do not emit radiation and are basically transparent to any thermal radiation. CO_2 and H_2O however, are polar molecules which emit and absorb thermal radiation over a wide temperature range. Most molecules are electrically polarized by positive charges separated from the negative charges. When the molecules rotate or vibrate the charges accelerate in a periodical fashion, and a sinusoidal oscillating train of electromagnetic waves is emitted. Molecules may be thought of as complex resonant harmonic systems with a large number of harmonic frequencies. When a molecule vibrates at a harmonic frequency it emits radiation, so that the frequency distribution of emitted radiation consists of spectral lines at these harmonic frequencies. Theoretically the lines would be very thin, occurring only at a single wavelength, but due to interaction between molecules, the Doppler effect and energy radiation, the lines are broadened. The three line broadening effects are:

- Doppler line broadening, caused by the translational movement of molecules and the Doppler effect.
- Collision line broadening, caused by collisions between molecules
- Natural lifetime broadening, caused by the decreased oscillation amplitude due to the energy radiated.

This is what gives the emission spectrum its shape.
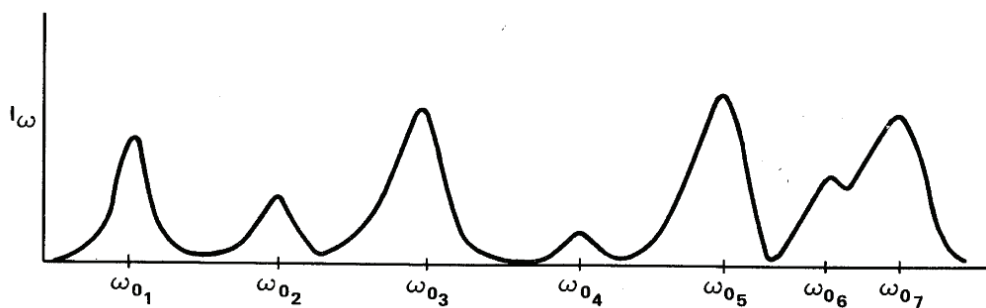
Figure 4 Example of emission spectrum of radiating gas [8]

Calculation of the radiative heat flux from a gas to a surface is complicated, but a simplified procedure may be used. This method was developed by Hottel [9] and involves radiation from a hemisphere onto a surface located at the base and center of the hemisphere. Emission from the gas to the surface is expressed as

$$E_g = \varepsilon_g \sigma T_g^4 \tag{2.28}$$

ε_g is the gas emissivity, and is taken from empirically obtained data. Values for emissivity of water vapor and carbon dioxide are plotted for gas temperature, partial pressure and hemisphere radius for a total pressure of 1atm. For other pressures, the emissivity must be multiplied by a correction factor C_w or C_c. If the gas is a mixture of water vapor and carbon dioxide, ε_g is obtained from the formula.

$$\varepsilon_g = \varepsilon_w + \varepsilon_c - \Delta\varepsilon \tag{2.29}$$

$\Delta\varepsilon$ is plotted for gas temperature, partial pressure and hemisphere radius. For other gas geometries the radius L may be replaced by a value called mean beam length, L_e. Using this method the radiative heat transfer from a gas to a surface A_s can be calculated by the formula

$$q = \varepsilon_g A_s \sigma T_g^4 \tag{2.30}$$

If the surface is a black surface at temperature T_s, the net radiation exchange may be expressed by

$$q_{net} = A_s \sigma (\varepsilon_g T_g^4 - \alpha_g T_s^4) \tag{2.31}$$

The gas absorptivity α_g is evaluated from the expressions

$$\alpha_w = C_w \left(\frac{T_g}{T_s}\right)^{0,45} \times \varepsilon_w \left(T_s, p_w L_e \frac{T_s}{T_g}\right) \tag{2.32}$$

$$\alpha_c = C_c \left(\frac{T_g}{T_s}\right)^{0,65} \times \varepsilon_c \left(T_s, p_c L_e \frac{T_s}{T_g}\right) \tag{2.33}$$

and

$$\alpha_g = \alpha_w + \alpha_c - \Delta\alpha \tag{2.34}$$

Values can be obtained from Hottels [9] charts

2.4.3   Emission from excited OH radicals

In much the same manner as CO_2 and H_2O molecules emits radiation at certain wavelengths, OH radicals from reactions in the combustion zone emit radiation as well. Excited OH radicals, OH*, can be formed by the reaction

$$CH + O_2 \rightarrow CO + OH*$$ (2.35)

in the primary combustion zone. Other possible reactions are

$$O + H \rightarrow OH*$$
$$H + O_2 \rightarrow OH* + O$$ (2.36)

The spectrum of OH* radicals is shown in Figure 5.
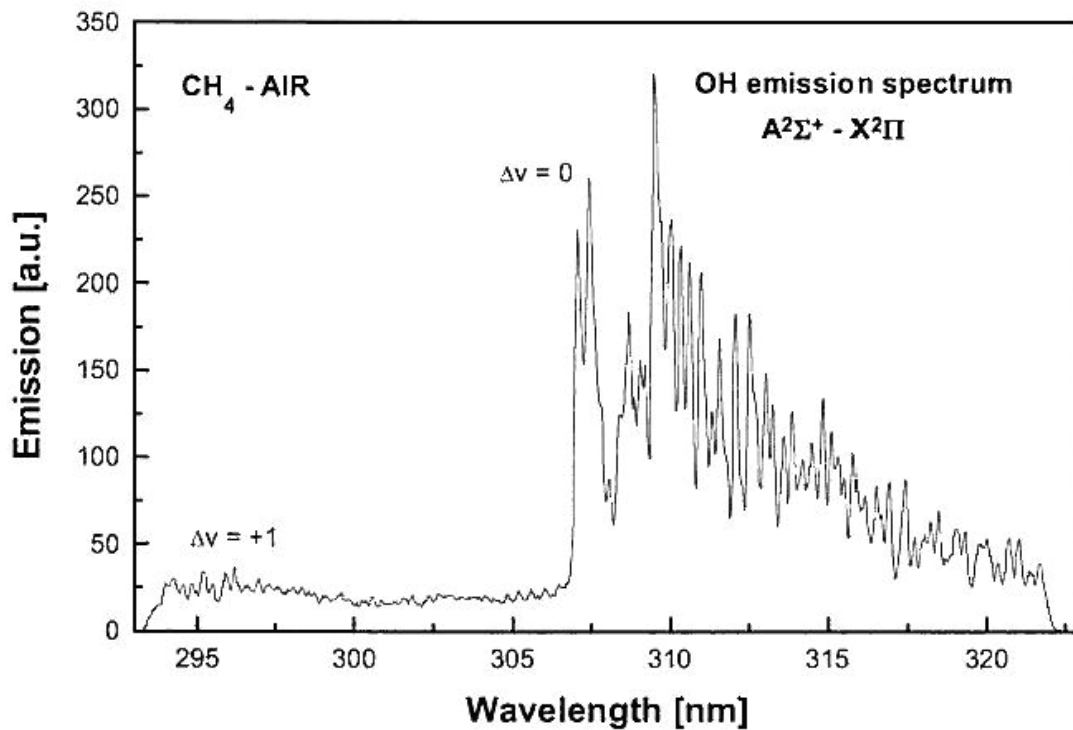
Figure 5 OH spectrum in lean premixed methane-air flame [10]

OH* radicals emit the strongest radiation at 306.4 nm, using optic filters that only let these wavelengths through, images can be taken of OH* radicals.

De Leo [11] performed experimental investigations on counterflow diffusion flames, and measured OH* and CH* concentrations. Figure 6 shows the results from a methane/air flame with 50% oxygen content and a strain rate of 30 s^{-1}. It is seen that OH* radicals exist mainly at the position of maximum temperature.
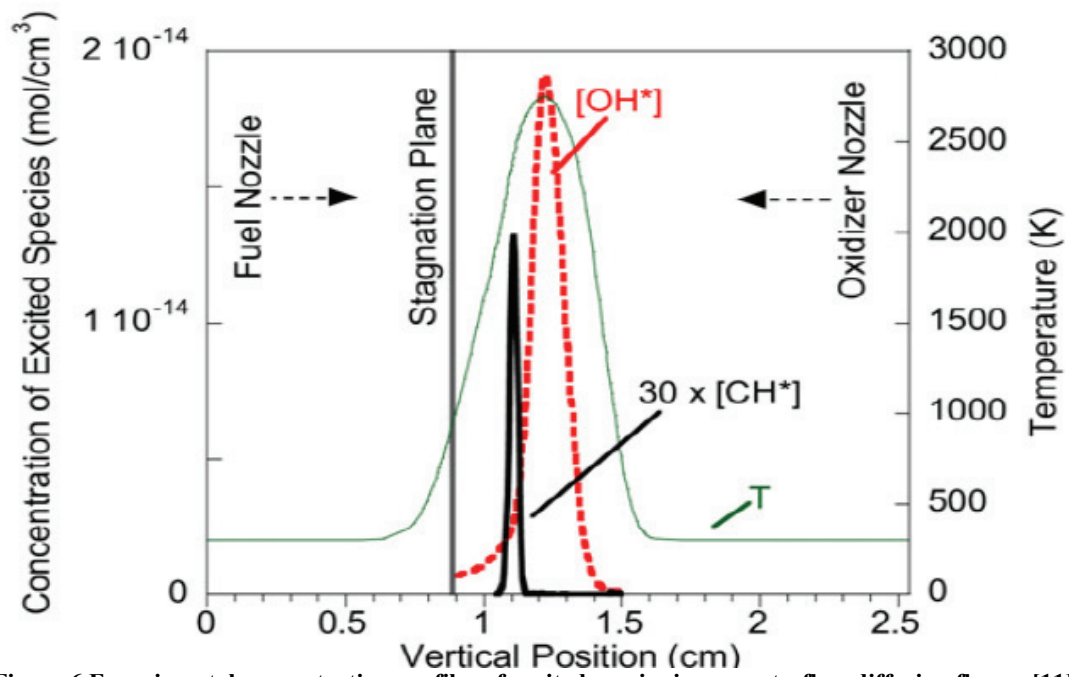
Figure 6 Experimental concentration profiles of excited species in a counterflow diffusion flames [11]

Thus, using imaging techniques that filter out OH* radicals, images of the combustion zone can be obtained.

2.5 FLAMES

One definition of a flame is [4]; " A flame is a self-sustaining propagation of a localized combustion zone at a subsonic velocities"

2.5.1 Non-premixed flames

Non-premixed flames are also known as diffusion flames. They usually consist of a jet of fuel issued from a pipe or tube into an oxidizing environment, typically air. The fuel and oxidizer are mixed by diffusion, and reacts in a thin reaction zone. At the centerline of the reaction zone the mixture is stoichiometric. Since the chemical reactions occur much faster than the diffusion, the speed of diffusion is the limiting factor of combustion.

The non-premixed flame is the most widespread flame in practical applications. Jet engines, diesel engines and hydrogen-oxygen rocket engines all make use of the non-premixed flame in some way. Since fuel and oxidizer remain separated until the combustion occurs, non-premixed flames are safer to handle than premixed flames. [6]

2.5.2 Premixed flames

In premixed flames the reactants are mixed molecularly in the stream. The flame will usually have conical shape, which is governed by the flow velocity and the laminar flame speed. If the mixture is fuel rich the flame is said to be partially premixed, and a secondary diffusion flame will occur downstream of the premixed flame.

2.5.3 Flame Length

The flame length can be defined as the axial location at the center of the jet ($r = 0$), where the equivalence ratio is unity ($\Phi = 1$). For flickering turbulent flames this height can be difficult to measure precisely, and a time average may be used.

For diffusion flames in a quiescent environment, there are four primary factors that determine the flame length [4]

- Relative importance of initial jet momentum flux and buoyant forces acting on the flame.
- Stoichiometry.
- Ratio of nozzle fluid to ambient gas density
- Initial jet diameter

In a simplified analysis of the laminar diffusion flame, one can ignore the effects of heat released by the reaction, and use a crude approximation to find the flame length, L_f.

$$L_f \approx \frac{3}{8\pi} \frac{Q_F}{DY_{F,stoic}} \qquad (2.37)$$

Here Q_F is the volumetric flow rate of fuel, D is the binary diffusion coefficient and $Y_{F,stoic}$ is the fuel mass fraction at stoichiometry.

When the non-premixed flame enters the turbulent regime, turbulent diffusion increases the mixing of molecules drastically leading to a shorter flame. Many correlations have been proposed for turbulent diffusion flame lengths.

2.5.4   Flame Speed

The laminar flame speed S_L for premixed flames is the speed at which the combustion process propagates through space, i.e. if you ignite a pipe filled with premixed air and methane, the flame front will propagate at a given speed. If the fluid in the pipe moves in the opposite direction of the flame front at a given velocity, the flame will stabilize at a fixed position. Since the viscous forces in a fluid causes velocity to be higher in the centerline of a pipe than close to the wall, the flame will get a conical shape. Laminar flame speed is defined mathematically as

$$S_L \equiv \dot{m}'' / \rho_u \qquad (2.38)$$

where $\dot{m}''$ is the mass flux [kg/m²-s] and ρ_u is the unburned gas density. To calculate S_L we can use the following equation

$$S_L = \left[-2\alpha(v+1)\frac{\bar{\dot{m}}'''_F}{\rho_u} \right]^{\frac{1}{2}} \qquad (2.39)$$

Here α is the thermal diffusivity, $\bar{\dot{m}}'''_F$ is the average mass production rate of fuel [kg/m³-s] and $(v+1)$ is stoichiometric coefficient on a mass basis

 If the flow is turbulent, the flame speed S_t is defined as "..the velocity at which unburned mixture enters the flame zone in a direction normal to the flame.." [4] and can be expressed by

$$S_t = \frac{\dot{m}}{\bar{A}\rho_u} \qquad (2.40)$$

Where $\dot{m}$ is the reactant flow rate, ρ_u is the unburned gas density, and $\bar{A}$ is the time averaged flame area.

For diffusion flames, flame speed has no physical meaning, .

2.5.5 Oxy-Fuel Combustion

Oxy-fuel combustion means using pure oxygen, or oxygen diluted with CO_2, as oxidizer. When the oxygen concentration is increased the reaction rate also increases, which means higher flame temperature and flame speed (Figure 7), and a decreased flame height. Because of the high temperatures associated with oxy-fuel combustion, it has been used a in glassmaking and with acetylene in blow torches for cutting steel. However, more recently the demand for CO_2 free power production has sparked an interest in applying oxy-fuel technology to coal and gas fired power plants.

The advantage of using oxy-fuel combustion in power plants with CO_2 seperation lies in the simplicity of removing CO_2 from the exhaust gas. Since the only products in the oxy-fuel combustion process are H_2O and CO_2 all that is needed for separation of CO_2, is to condense the water vapor. And because no nitrogen is present, there is no NO_x pollution either. The drawback compared to power plants without CO_2 removal is lower efficiency since power is needed for air separation and CO2 sequestration, cooling and compression.
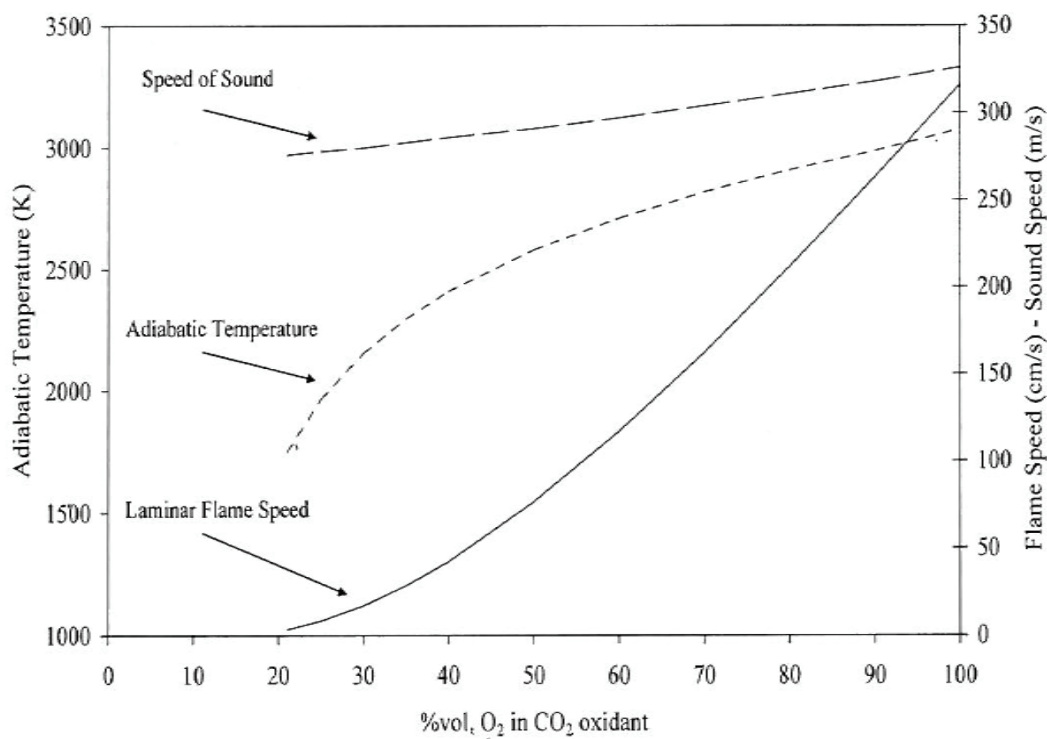
Figure 7 Calculated adiabatic temperature, flame speed and sound speed for methane burning in O2/CO2 under stoichiometric conditions [12]

The change in combustion properties for an oxy-fuel flame can be seen in Figure 7. An air/methane mixture has a laminar flame speed of approximately 39 cm/s, which corresponds to an O2 concentration of nearly 40% which again would yield an adiabatic flame temperature of 2400K, about 200K higher than for air. This is due to the higher thermal conductivity and lower density of nitrogen compared to CO2 [12].

Examples of oxy-fuel flames with varying O_2 concentrations are shown in Figure 8. The flame is clearly shorter and more intense at higher oxygen concentrations.
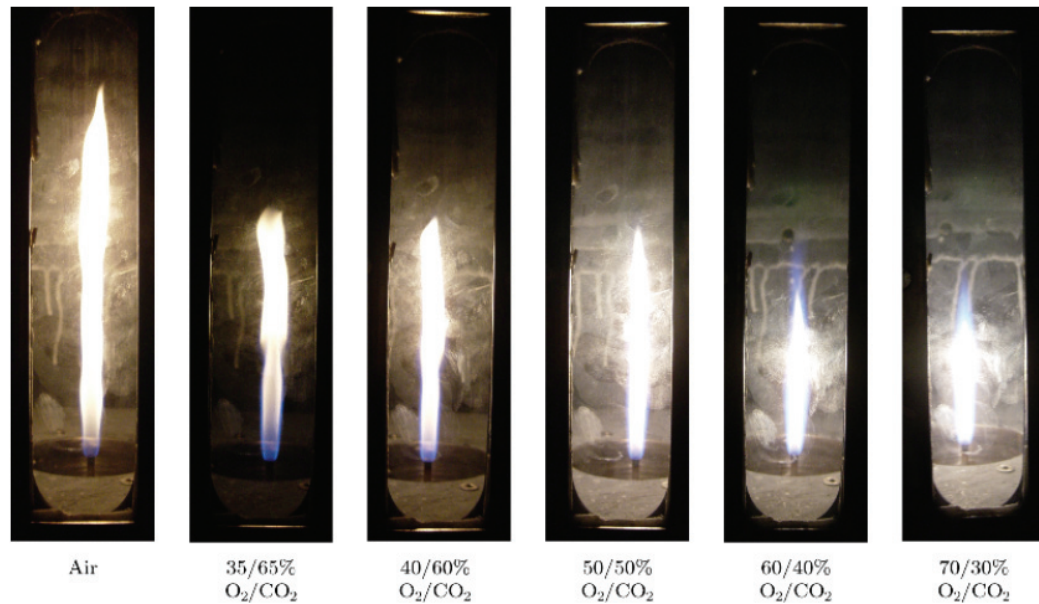
Figure 8 1kW flame in various oxidant environments [13]

Higher concentrations of CO_2 and H_2O results in higher gas emissivities, potentially causing material damage to the combustion chamber[14]. Oppelt [13] conducted experiments on the radiative heat transfer from oxy-fuel flames, the results for a 2kW flame are shown in Figure 9. It is seen that the O_2 concentration has a significant effect on the heat flux.
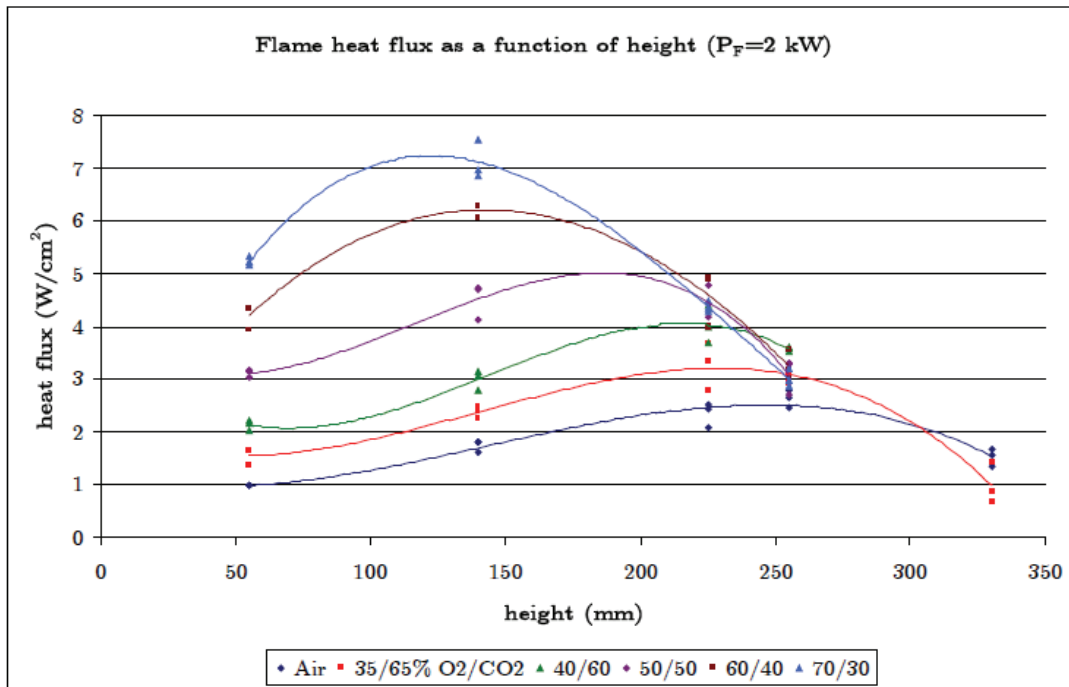
Figure 9 Heat flux from a 2kW flame at different heights from the jet exit [13]

2.6 LIFT-OFF

As the velocity of fuel in a non-premixed flame is increased, and thus the Reynolds number increases, the flame becomes turbulent. If the jet velocity is increased even more, the flame eventually detaches from the pipe and stabilizes a number of pipe diameters downstream. Flames at this state are called lifted diffusion flames, the distance between the duct and the flame base is called lift-off height, and the velocity at which the detachment occurs is called the lift-off velocity. If the velocity is increased furthermore it will result in flame blowout. It is possible for certain fuels to detach and maintain a lifted flame while in the laminar regime [15], an important parameter in this case is the Schmidt number, Sc , a measure of kinematic viscosity to mass diffusion. Lifted laminar jet diffusion flames are not possible for $0,5 < Sc < 1,0$, but they have been observed with propane as fuel, $Sc = 1,3$ [2].

Lift off is dependent on several different parameters. Kalghatgi [16] did extensive experimental research and found that the lift-off height increases linearly with jet velocity, is independent of nozzle diameter, and inversely proportional to the maximum laminar flame speed. Hence lift-off is also dependent on fuel type, since the laminar flame speed varies for different fuels.

2.6.1 Effect of nozzle geometry

Iyogun and Birouk [17] investigated the use of asymmetric fuel nozzles, and showed that the asymmetric nozzles reduces the lift-off height, and influences the lift-off, blow-off and reattachment velocities. This was explained by the higher entrainment rates in jets from asymmetric nozzles which indicate improved mixing. As can be seen in Figure 10, the triangular nozzle has the lowest lift-off height at velocities below 43 m/s, and the rectangular nozzle exhibits the lowest lift-off height for velocities above 43 m/s.
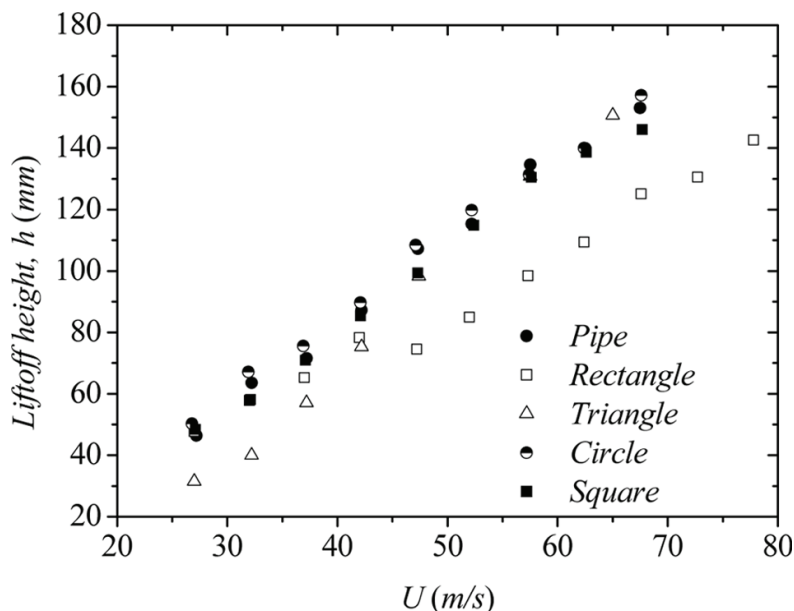

Figure 10 Lift-off height vs jet velocity for various geometries [17]

2.6.2 Effect of co-flow velocity

Lift-off and blow-out velocities are affected by the co-flow velocity as well. Leung and Wierzba [18] investigated the effect of co-flow velocity on lift-off characteristics, and found a clear connection between the co-flow velocity and lift-off, blowout and blowoff. Four distinct regions can be observed in Figure 11. In region I the lift-off and blowout velocity increases with higher co-flow velocity, this behavior of the blowout limit may be affected by shortage of oxidizer for the lowest co-flow velocities. At a co-flow velocity of approximately 0.09 m/s the blowout velocity decreases with higher co-flow velocity, while the lift-off velocity continues to increase (region II). Region III starts at about 0.23 m/s at witch point an attached flame ignited at low velocities would blowoff directly as the fuel speed increased. However, a flame ignited at higher velocities would stabilize as a lifted flame, in this case it would experience blowout at high velocities. For co-flow velocities above 0.9 m/s no stable lifted flames could be obtained, and attached flames would proceed directly to blowoff (region IV).
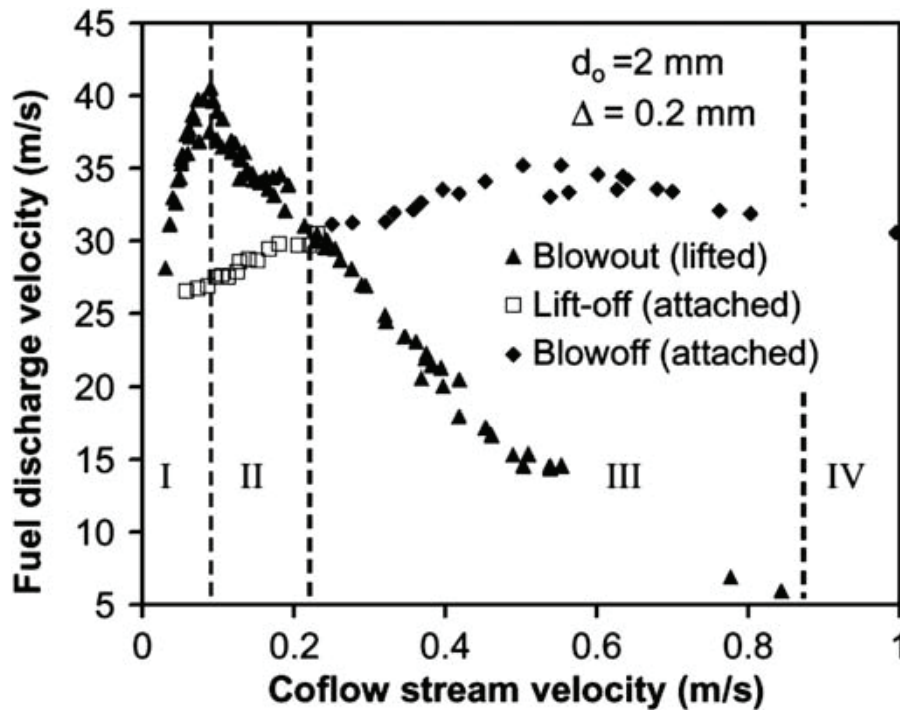

Figure 11 Lift-off, blowoff and blowout velocities vs co-flow velocity [18]

2.6.3 Theories on the behavior of lifted turbulent jet diffusion flames

The lifted turbulent jet diffusion flame has been the subject of numerous research papers, but none of the theories available are satisfactory in describing the flame stabilization according to Lyons [2] and Pitts [3].

Premixed theory

Vanquickenborne and Van Tiggelens research [19] proposed that the lifted flame base is premixed, and burns with a turbulent burning velocity. The premixed flame is stabilized at the point where the gas velocity is equal to the burning velocity, (Figure 12, II). At any point above the flame base (y >H_B) (Figure 12, I), the gas velocity is lower than the turbulent flame speed over the width Δx . Below the flame base (y < H_B) (Figure 12, III) the gas velocity is always higher than the turbulent flame velocity. This is also illustrated in Figure 13(a), where the premixed region is the shaded surface, the boundaries are the upper and lower flammability limits. A three-dimensional proposed model of the lifted flame is sketched in Figure 13(b), it can be seen that downstream of the flame base the flame behaves as a diffusion flame. This is coherent with the edge flame theory. Newer experimental research has shown that the premixing is not extensive enough to support this theory alone, and that it should be supplemented by the effect of large scale structures in the jet [2].
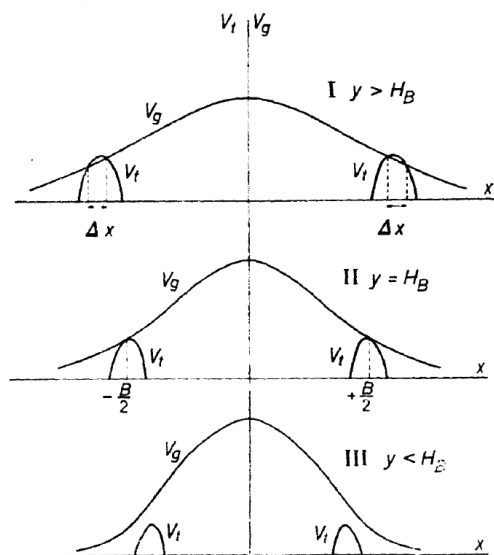

Figure 12 Fuel velocity (V$_G$) and turbulent flame speed (V$_T$) at three different heights y [19]
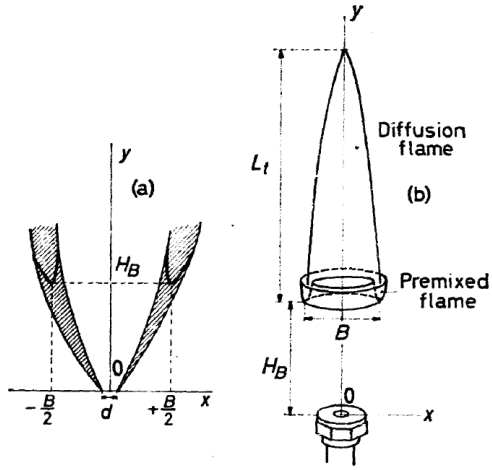
Figure 13 Vanquickenbornes proposed model for lifted flames [19]

Kalghatgi [16] developed a correlation for lift-off height using the premixing theory

$$\frac{hS_L}{v_e} = C_2 \left(\frac{U_e}{S_L}\right)\left(\frac{\rho_e}{\rho_\infty}\right)^{1,5} \tag{2.41}$$

Critical scalar dissipation

Peters and Williams [20] proposed that extinction of diffusion flamelets controls the flame stabilization. The scalar dissipation rate, X, was used to scale the lift-off height. Lift-off is said to occur when the scalar dissipation rate at stoichiometry equals the scalar dissipation rate at extinction, $X_{st} = X_{qu}$. A theory which scales the dissipation rate at extinction with the global residence time, d/U, was formulated as

$$X_{qu}^* = X_{qu}\left(d/U\right) \tag{2.42}$$

And this formula was then used to develop three theories relating the non-dimensional scalar dissipation rate to nozzle diameter and lift-off height.

$$X_{qu}^* = X_{tb1} = 0,24(d/h)^{1,5}(1-0,096\sqrt{h/d}) \tag{2.43}$$

$$X_{qu}^* = X_{tb2} = 0,46(d/h)^2(1-0,039(h/d)^{\frac{1}{1,4}}) \tag{2.44}$$

$$X_{qu}^* = X_{tb3} = 0,018(d/h) \tag{2.45}$$

X_{tb1} and X_{tb3} are both derived from the formula for the non-dimensional scalar dissipation rate, but X_{tb3} was manipulated to produce better agreements with data on lift-off heights. X_{tb2} uses a slightly different approach. As can be seen in Figure 14 the third theory is in good agreement with experimental data, and the two other theories are in the right order of magnitude. The X_{qu}^* line was made from experimental data points, using equation with $X_{qu}=5\ s^{-1}$

- 23 -
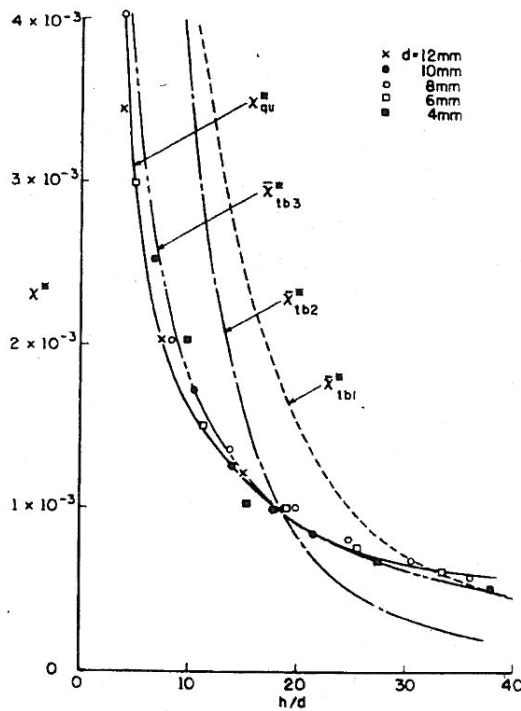
Figure 14 Non-dimensional scalar dissipation rate vs ratio of lift-off height to jet diameter [20]

The paper is a theoretical analysis, yet the predictions are in good agreement with experimental data on methane flames. It was argued that molecular premixing could not occur at a substantial amount. Using typical lift-off heights of 3 to 30 cm and exit velocities of 10 to 60 m/s it was calculated that the typical residence time for fuel elements prior to entering the combustion zone was 1 to 5 ms. Using these numbers it was calculated that molecules could diffuse about 10^{-2} cm in the time available, that 50 to 90 % of the diffusion occurred in the smallest eddies, and it seemed unlikely that a sufficient amount of premixing occurs to justify the premixed-flame concept. This conclusion has been the major argument against the theory, since there is experimental evidence to prove that premixing actually does occur. Figure 15 shows the concentration fluctuations in a stream of propane at Re = 3960. Red indicates a combustible mixture, blue and white represent fuel lean and fuel rich mixture. It can be seen that mixing does occur, but not enough to create a stabilized lifted flame.

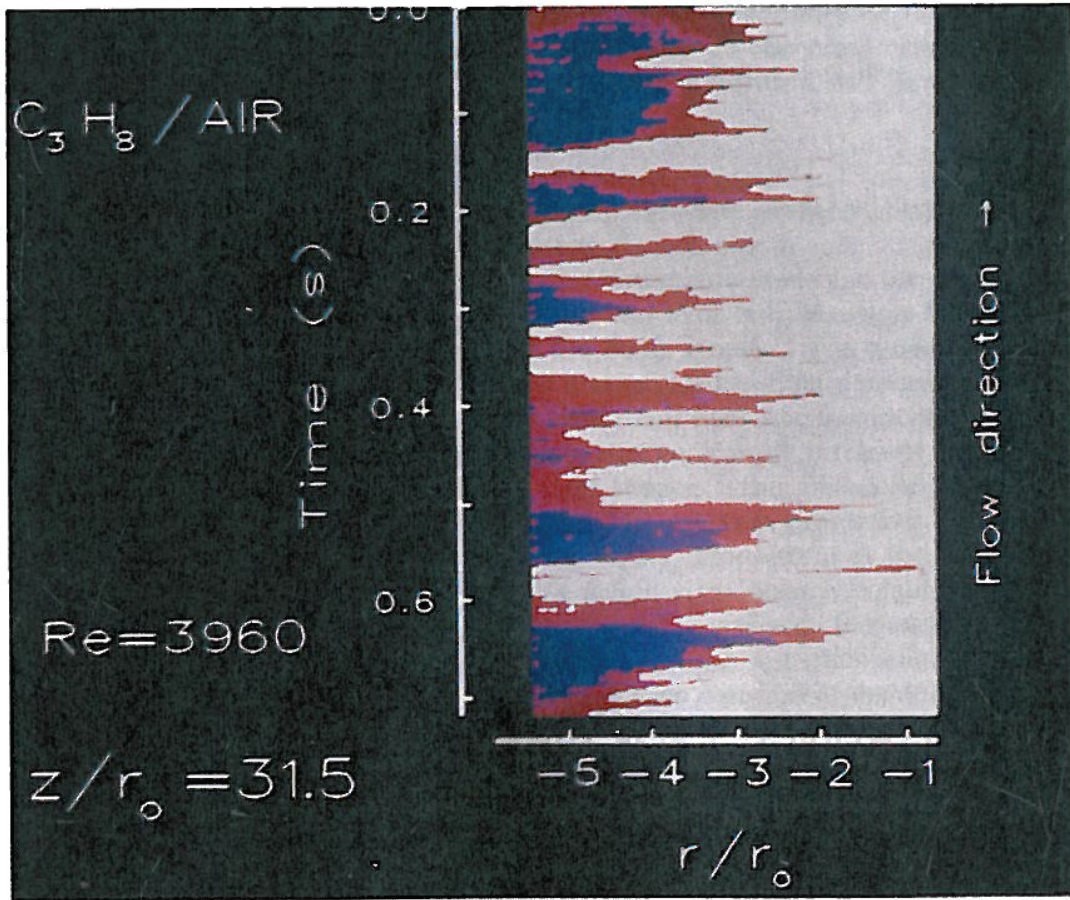**Figure 15 Space-time plot of propane concentration at h/r= 31.5 [3]**

Edge-flame concept

The edge-flame concept is based on partial premixing upstream of the flame base. This theory has been thoroughly researched the last couple of decades and is consistent with the triple, or tribrachial, flame structure which has been shown experimentally and analytically [2]. The partially premixed flame edge burns with two fronts, a fuel rich flame on the side facing the jet, and a fuel lean flame on the side facing the oxidant, remaining fuel is burnt in a trailing diffusion flame further downstream (Figure 16), hence the term triple-flame. Most research on triple-flames has been done in laminar jets, but the research is being extended to include turbulent flow as well. Figure 17 is taken from an experimental study by Joedicke et.al [21]. The study reports experimental observation of all three triple flame branches in turbulent flowfield. The images supposedly show a) the temperature field, b) lean premixed combustion, c) diffusive combustion and d) rich premixed combustion. Image a) was made using Rayleigh imagery, b) utilized laser induced fluorescence (LIF) of CH_2O c) used LIPF of OH and d) LIF of PAH images.
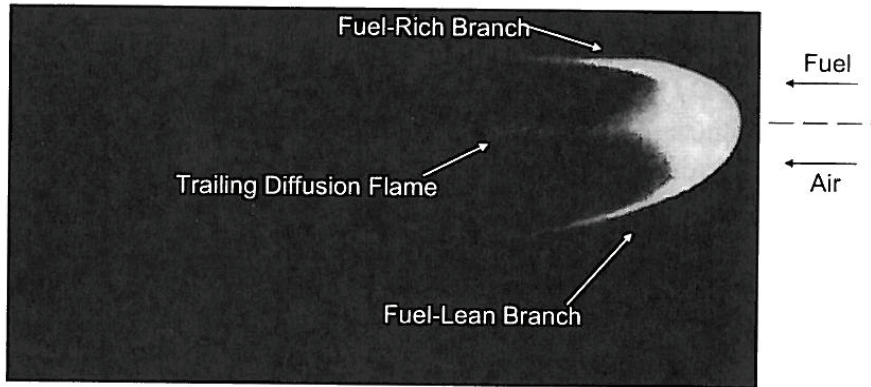
Figure 16 Triple flame structure in a lifted laminar jet diffusion flame[2].
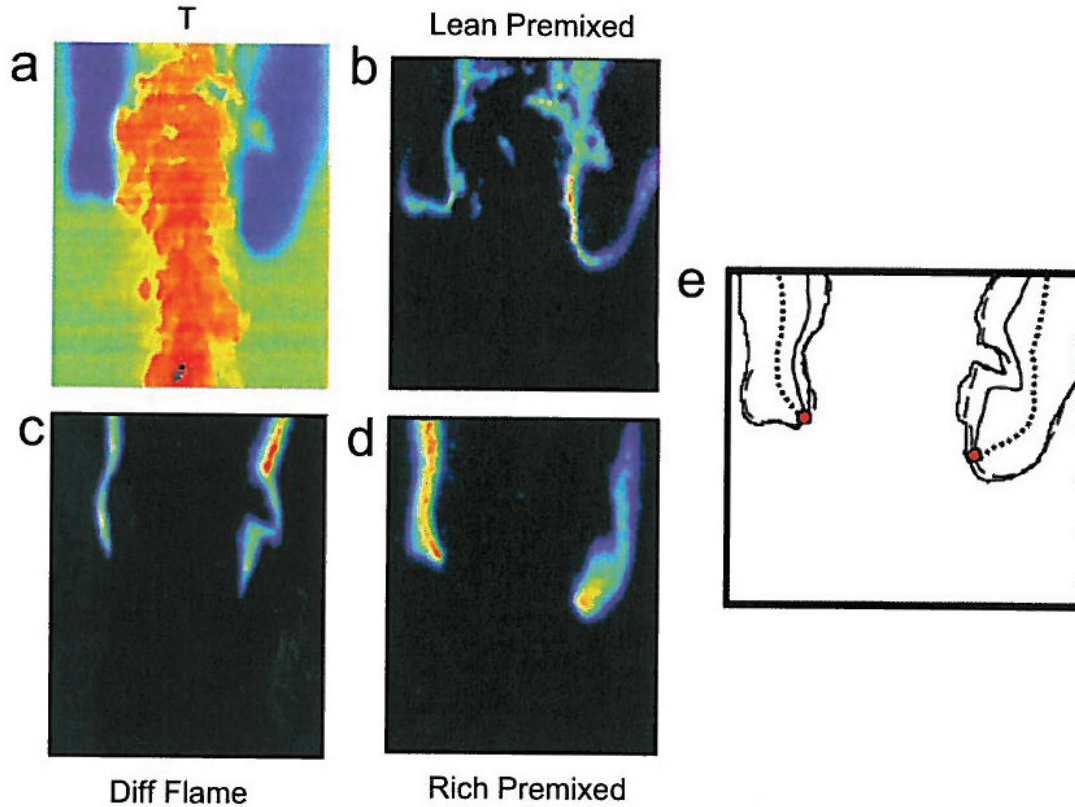
Figure 17 Sample of a) Rayleigh b) LIF of CH2O c) LIPF of OH and d) LIF of PAH images. The contours obtained from Rayleigh and reaction zones loci obtained from each LIF signal are shown in each image and then combined in e) to argue [21]

Large eddy concept

Other scientists [22, 23] argue that the large scale structures in turbulent jets are important in flame stabilization. That is, hot downstream products are transported upstream by large eddies to maintain the flame base. However this is largely unsupported by experimental evidence [2]. The theory is sometimes used in association with the premixed and edge-flame theories.

2.6.4 Hysteresis

With regards to flame lift-off, hysteresis means that the lift-off velocity is higher than the reattachment velocity. This phenomenon has been well documented experimentally and is thought to be caused by increased turbulence in the cold flow region below the lifted flame which again causes higher velocities of entrained air at the lifted flame base [24].

2.6.5 Lift-off in oxy-fuel flames

To the writers knowledge there have not been any experimental investigations published regarding lift-off characteristics for flames burning in oxy-fuel environment. However, experiments on oxygen enriched combustion indicates shorter flames, stabilized closer to the jet exit, with increasing oxygen enrichment [25]. If the premixing theories are used to predict lift-off, it can be deducted that increasing laminar burning velocity would yield lower lift-off heights. This would indicate that increasing O_2 concentration would lead to lower lift-off heights.

3   METHOD

3.1   THE OXY-FUEL RIG

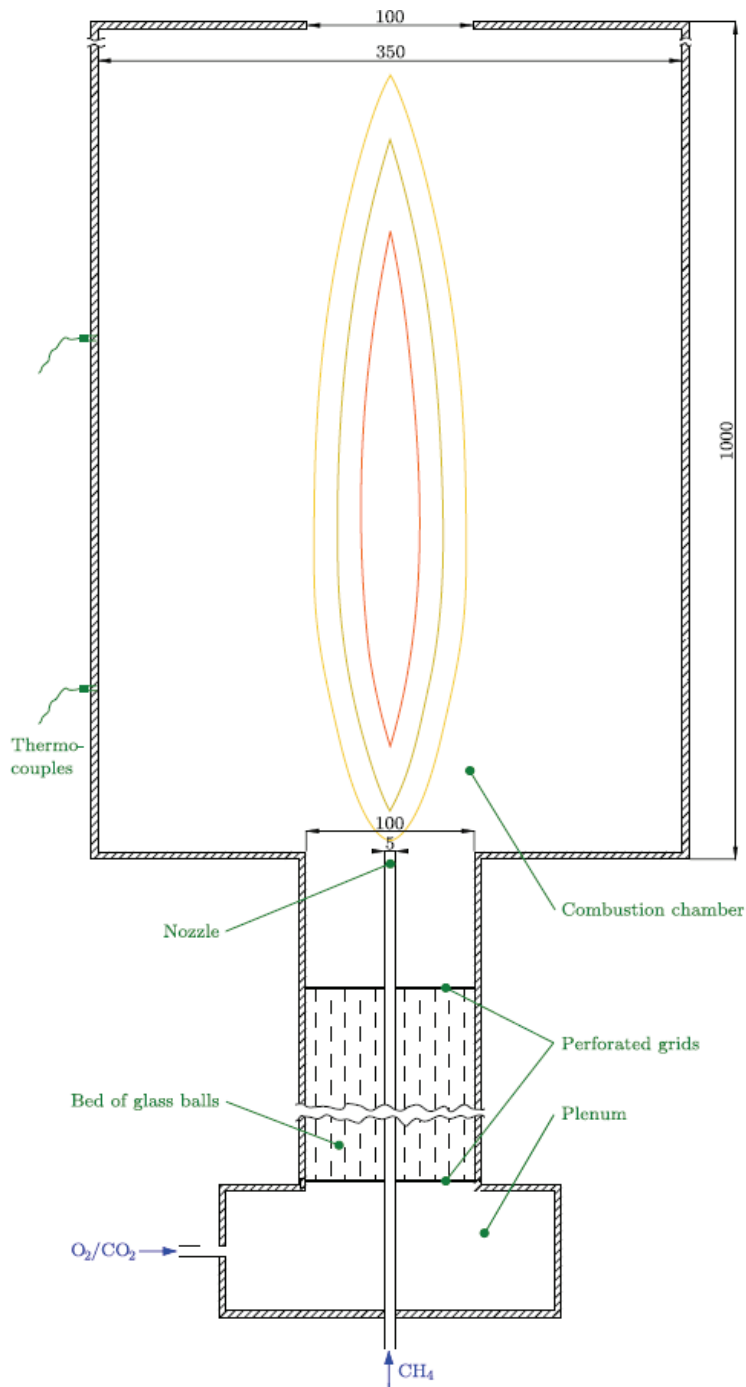The combustor used for all experiments in this study was the SINTEF rig for diffusion flames shown in Figure 18.

Figure 18 The SINTEF diffusion flame rig

The rig consists of the following parts:

- A thin walled stainless steel pipe with a diameter of 350mm used as a wall to prevent the coflow from being mixed with air. The large diameter ensured even large flames where not influenced. The wall was painted on the inside with a high-absorbing paint to absorb the maximum amount of heat from the flame
- Thermocouples welded on the wall at heights of 200mm and 500mm to allow measurements of wall temperature.
- Thermocouples in the plenum and just above the glass balls for gas temperature measurements.
- A plenum to ensure proper mixing of the coflow.
- A stainless steel tube with 100mm diameter for the coflow.
- A section filled glass balls, with perforated grids in each end, to make sure the flame was not influenced by swirl in the coflow stream.
- Three windows mounted on the chamber wall. One to allow pictures to be taken of the flame, another for IR flame-sensor, and the third to allow visual observation of the flame by the operator.
- Changeable stainless steel tubes with an outer diameter of 6mm, and inner diameters of 2mm, 4mm and 5mm for the methane stream. Three different tubes were used to allow observation of a wide range of fuel velocity and Reynolds numbers. The tubes where tapered on the end to a thin lip (0.2mm – 0.5mm).

A photograph of the rig is shown in Figure 19
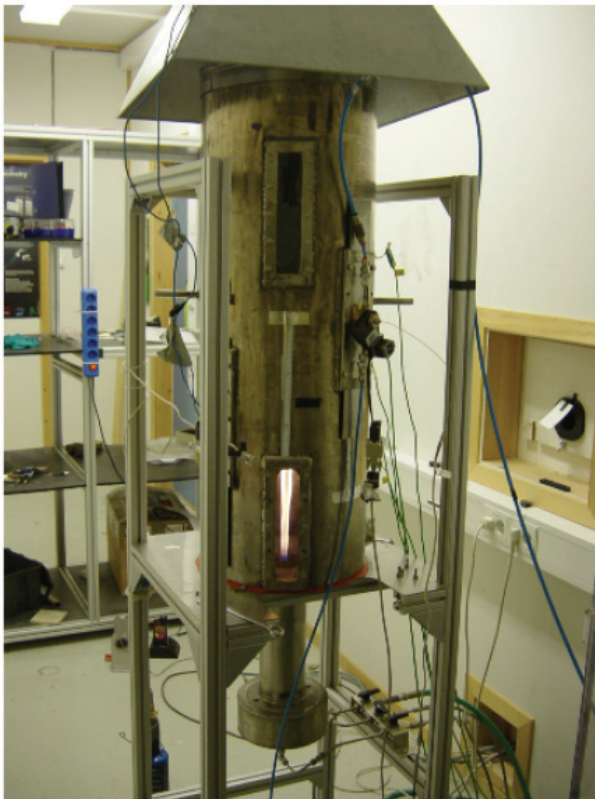
Figure 19 Photo of the SINTEF diffusion flame rig

Methane gas was delivered in 50 liter gas bottles at 150 bar. Oxygen and carbon dioxide were delivered from 50 and 40 liter bottles at 250 and 50 bars respectively. The oxygen and carbon dioxide streams used separate mass flow controllers to allow control of oxygen concentration in the coflow. Downstream of the mass flow controllers the coflow was merged into a single tube to allow proper mixing. Air was delivered from the compressed air plant. Figure 20 shows the schematics of the setup.
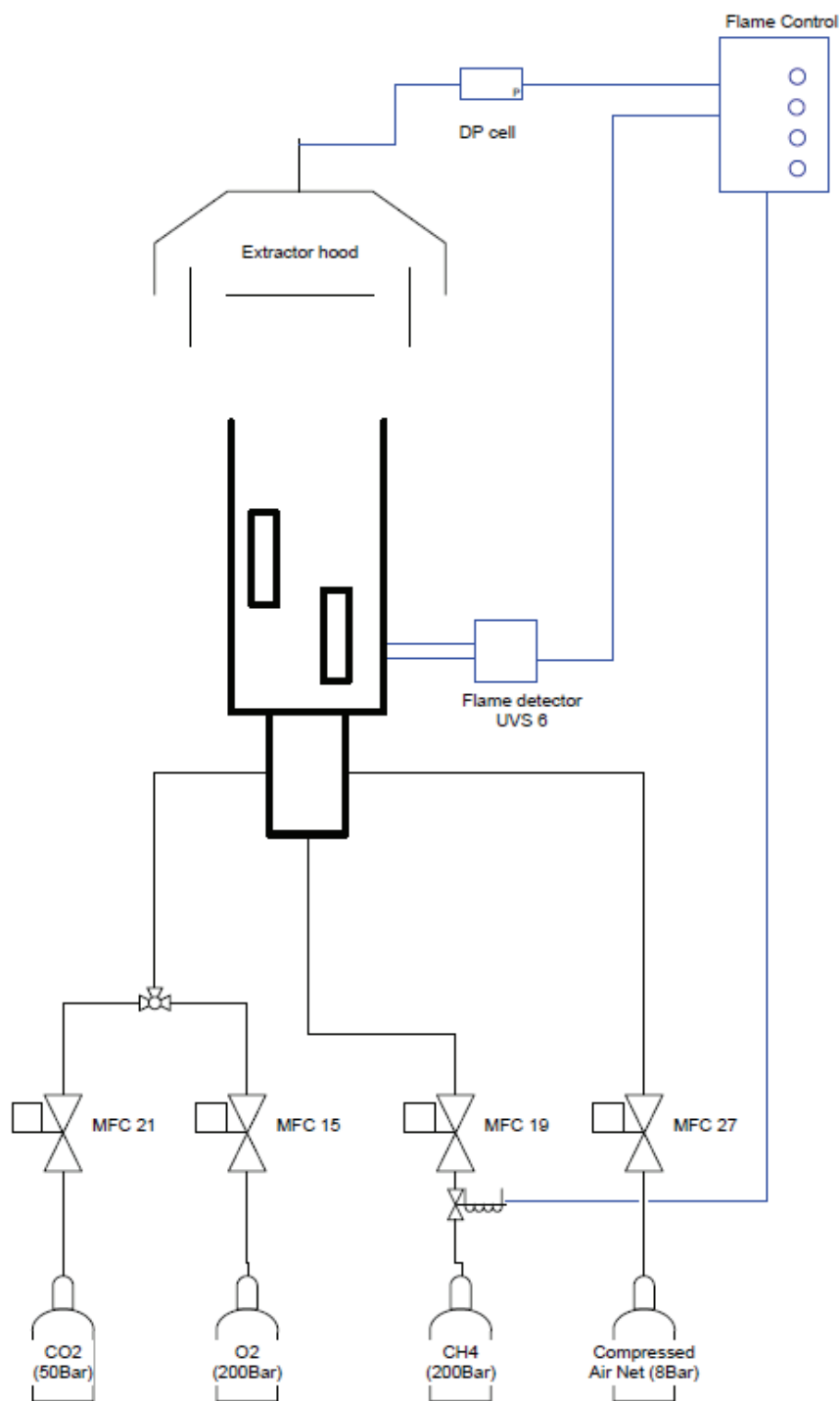

Figure 20 Laboratory setup

Brooks Instruments mass flow controllers were used to control all mass flows. Table 1 lists the different mass flow controller, their range and accuracy.

STREAM	Name	MODEL	RANGE		ACCURACY
O_2	MFC-15	Brooks Instruments	0-103,6	ln/min	0,7% of rate
CO_2	MFC-21	Brooks Instruments	0-192,6	ln/min	+ 0.2% of full
Air	MFC-27	Brooks Instruments	0-500	ln/min	scale
CH_4	MFC-19	Brooks Instruments	0-53,51	ln/min	

Table 1 Index of mass flow controllers used in experiment

Mass flows in table 1 are in normal liters pr minute. To calculate actual jet velocity, methane gas was assumed to be at 20° C and calculated from

$$\dot{m}_n = \dot{m}_a \Rightarrow \rho_n Q_n = \rho_a Q_a \tag{3.1}$$

Subscript n indicates normal conditions (1bar, 0° C), and a indicate actual conditions (1bar, 20° C). Using the perfect gas law, assuming $p_n = p_a$ and a compressibility factor of 1 we get

$$Q_a = \frac{\rho_n}{\rho_a} Q_n = \frac{\dfrac{p_n}{ZRT_n}}{\dfrac{p_a}{ZRT_a}} Q_n = \frac{T_a}{T_n} Q_n \tag{3.2}$$

And then, inserting $Q = V \cdot A$ in (3.2) we get the velocity as

$$V = \frac{T_a}{T_n} Q_n \frac{4}{\pi r^2} \tag{3.3}$$

The experimental measurements of lift-off heights where conducted using a CCD camera (FlameStar II, LaVision Gmbh) connected to a LaVision camera controller. The camera was operated using the DaVis software version 6.2.2 from LaVision. Adjustments of exposure width and intensity gain were done from the camera controller. For low intensity flames, typically low oxygen concentration in the co-flow and low power flames, a higher exposure width was necessary. However, the turbulence made it necessary to keep the exposure width as short as possible to allow for instantaneous images to be taken. A 307nm optic filter with a 10nm band pass was used on the camera objective so that only radiation from excited OH radicals was filtered through.

The thermocouples were connected to a Texas Instruments Control Box, which again was connected to a computer. Temperature measurements in the gas and on the combustion chamber wall were then logged using a visual basic program written by Mario Ditaranto.

Measurements were conducted in oxygen concentrations ranging from 34% to 50% with the co-flow kept at constant volumetric flow rate of 171,84 nl/min, corresponding to a velocity of 0,4 m/s.

It will be shown that the combustor wall temperature greatly affected the lift-off properties of oxy-fuel flames. In an effort to measure this influence, efforts were made to do lift-off measurements on various wall temperatures. This proved difficult since the presence of a flame naturally heats up the surrounding wall. Nevertheless, all measurements were tried to be conducted at cold, hot and medium chamber wall temperatures.

3.1.1 HSE

Safe operation of the rig was ensured by three independent safety features.

To prevent methane flow into the chamber without combustion, and thus filling up the chamber with large amounts of ignitable gas, an IR sensor was placed outside the chamber. The IR sensor was connected to a solenoid valve controlling the methane flow. When the propane burner used to ignite the flame was ignited inside the chamber, the IR sensor would open the valve and allow methane to enter the chamber and be ignited. If the velocity reach a level were the flame was blown out, the vale would close and prevent more methane from entering the chamber.

The second safety feature was a pressure sensor mounted on the ventilation above the combustion chamber. The pressure sensor would close the solenoid valve if the ventilation was turned off or too weak. This prevented the room from being filled up with exhaust gases if ventilation was insufficient.

Lastly an emergency button on the wall would close the valve if pushed.

3.2   MEASUREMENT OF LIFT-OFF HEIGHT

For each flame configuration 120 images were taken to capture fluctuations in the combustion. An example of two instantaneous images of a 12kW in a 34% O_2 environment is shown in Figure 21 to illustrate the fluctuations.
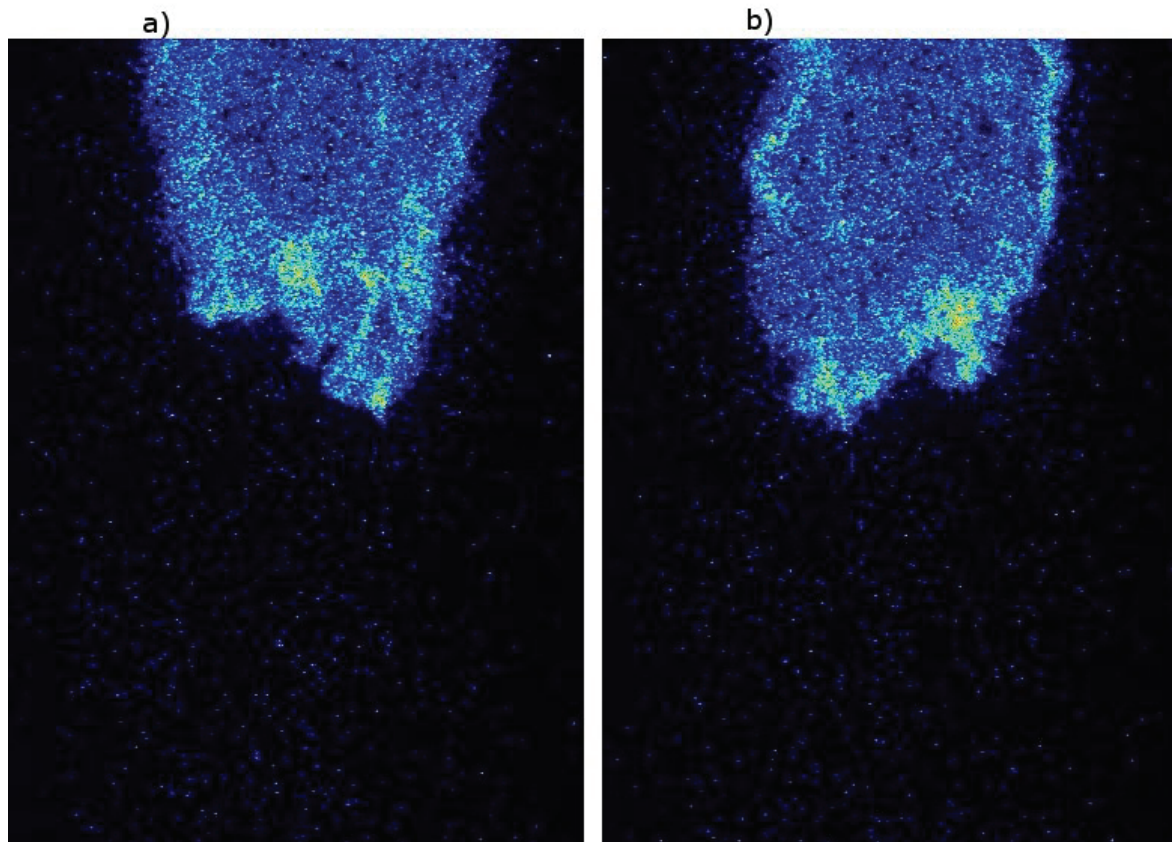
Figure 21 Two instantaneous images of a 12kW flame in a 34% O2 environment.

The lowest point of the flame moves from right in picture a) to left on picture b), and the position with the highest intensity is seen to move from the center in picture a) to right on picture b).

The imaging software was then used to process the instantaneous images into an average image as shown in Figure 22. The average image was used to find the maximum intensity, half of which was used as threshold in a PDF post processing of the images, the normalized PDF image is shown Figure 23. It can be seen that the normalized image has removed all the background noise, and it has an intensity range from 0 to 100. The lift-off height, h_{lo}, was then defined to be at an intensity of 50 in the normalized image, which means that the flame is present at that point, at intensity above the selected threshold, 50% of the time in the recorded images. To quantify the fluctuations, heights at 25% and 75% were also measured to make a Δh value.
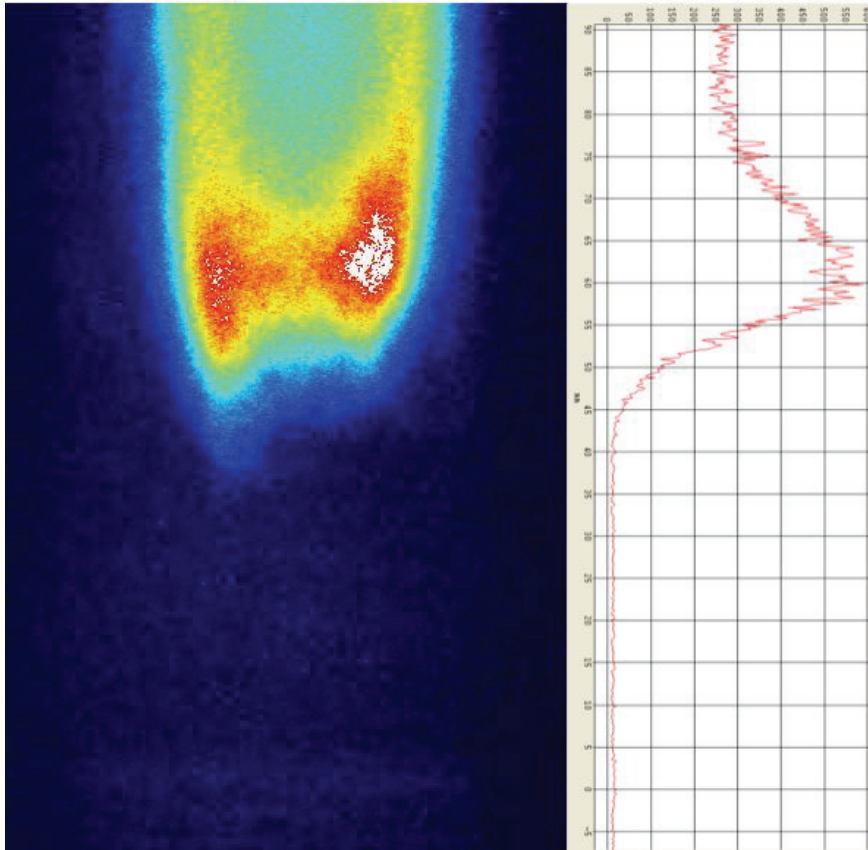
Figure 22 Average of 120 instantaneous images of 12kW flame in 34% O2 environment with intensity profile
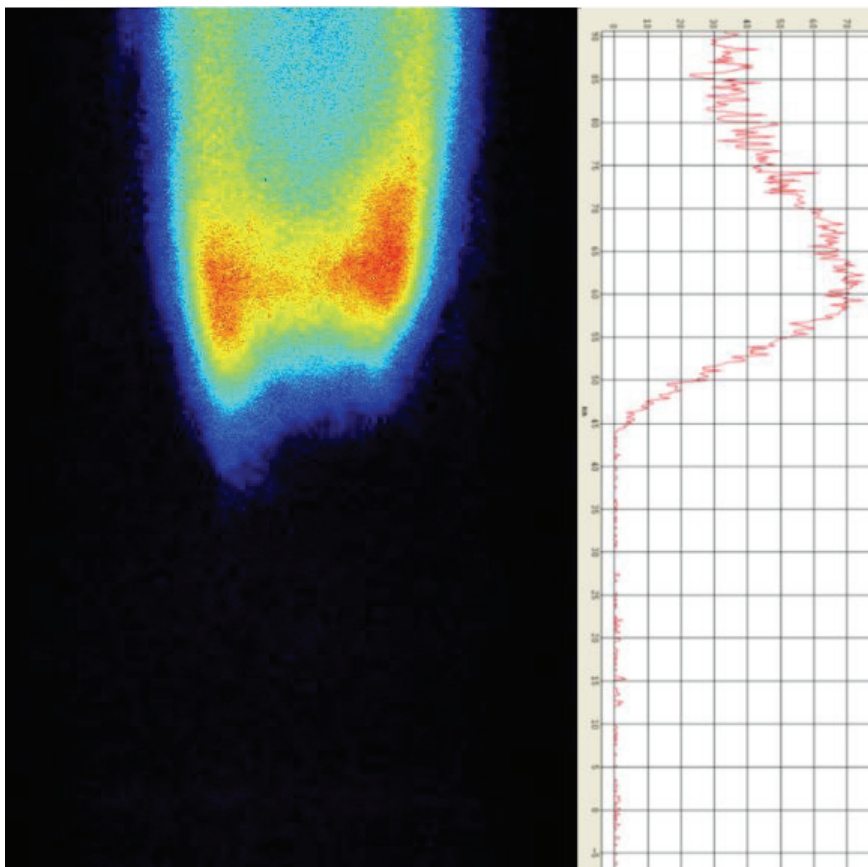

Figure 23 PDF normalized image of 12kW flame in 34% O2 environment with intensity profile

3.3 MEASUREMENT UNCERTAINTIES

As seen in table 1, the mass flow controllers have an accuracy of 0.7% of the flow rate + 0.2% of full scale flow rate. This leads to uncertainties in the flow rates through the MFCs. When calculating the jet exit velocities, it was assumed that the methane had a temperature of 20° C, however the temperature in the methane flow was not measured, so there are uncertainties.

The jet exit velocity is a function of the volumetric flow rate, the fluid density and the jet exit area, and the fluid density is dependent on temperature. Thus, the uncertainties regarding the gas temperature, and flow rate relates directly to uncertainties in the jet exit velocity.

Lift-off heights were measured from a normalized picture where a selected value was used as a threshold as explained in section 3.2. Assuming that this threshold was selected with an accuracy of 10% of max intensity, the uncertainty in can be found.

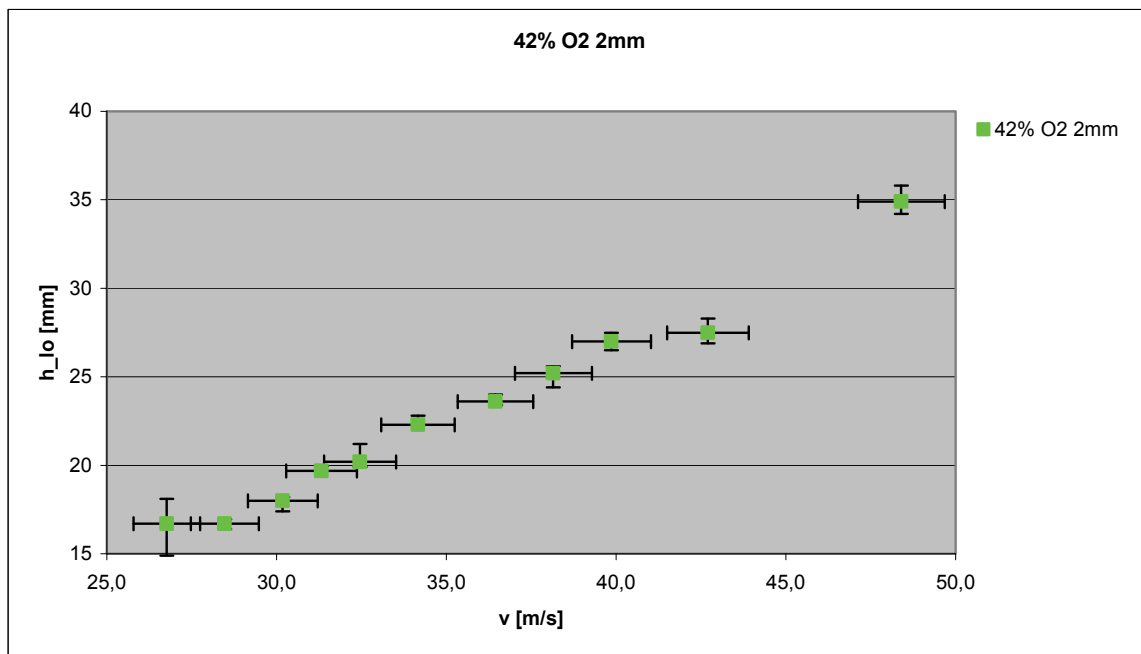Uncertainties for jet exit velocity and lift-off height are shown in Figure 24

Figure 24 Uncertainties for 2mm nozzle diameter and 42% oxygen concentration.

4 RESULTS AND DISCUSSION

4.1 EFFECT OF OXYGEN ENRICHED AIR ON LIFT-OFF CHARACTERISTICS

Experimental results of lift-off heights and velocities from measurements done with a methane jet in air and oxygen enriched air are shown in Figure 25. Experimental data from Ditaranto [26] and Kalghatgi [16] are also included for reference.

The measured values seem to differ slightly from the results of Ditaranto and Kalghatgi for CH_4 burning in air. There is a major difference between the experiments carried out in this report, and those of Ditaranto and Kalghatgi, namely the presence of co-flow. Ditarantos and Kalghatgis experiments were conducted in open air without co-flow and the effect of co-flow is shown to have a great effect on flame stability (ref. section 2.6.2).

It is seen clearly that an increase in oxygen concentration results in shorter lift-off heights, most likely due to the higher burning velocities associated with increasing oxygen concentration.

Since experiments were carried out in an enclosed chamber with a constant flow of oxidants, oxygen depletion may occur for the more powerful flames, thus altering the flame characteristics. The effects of oxygen depletion on lift-off characteristics have not been investigated in this report.
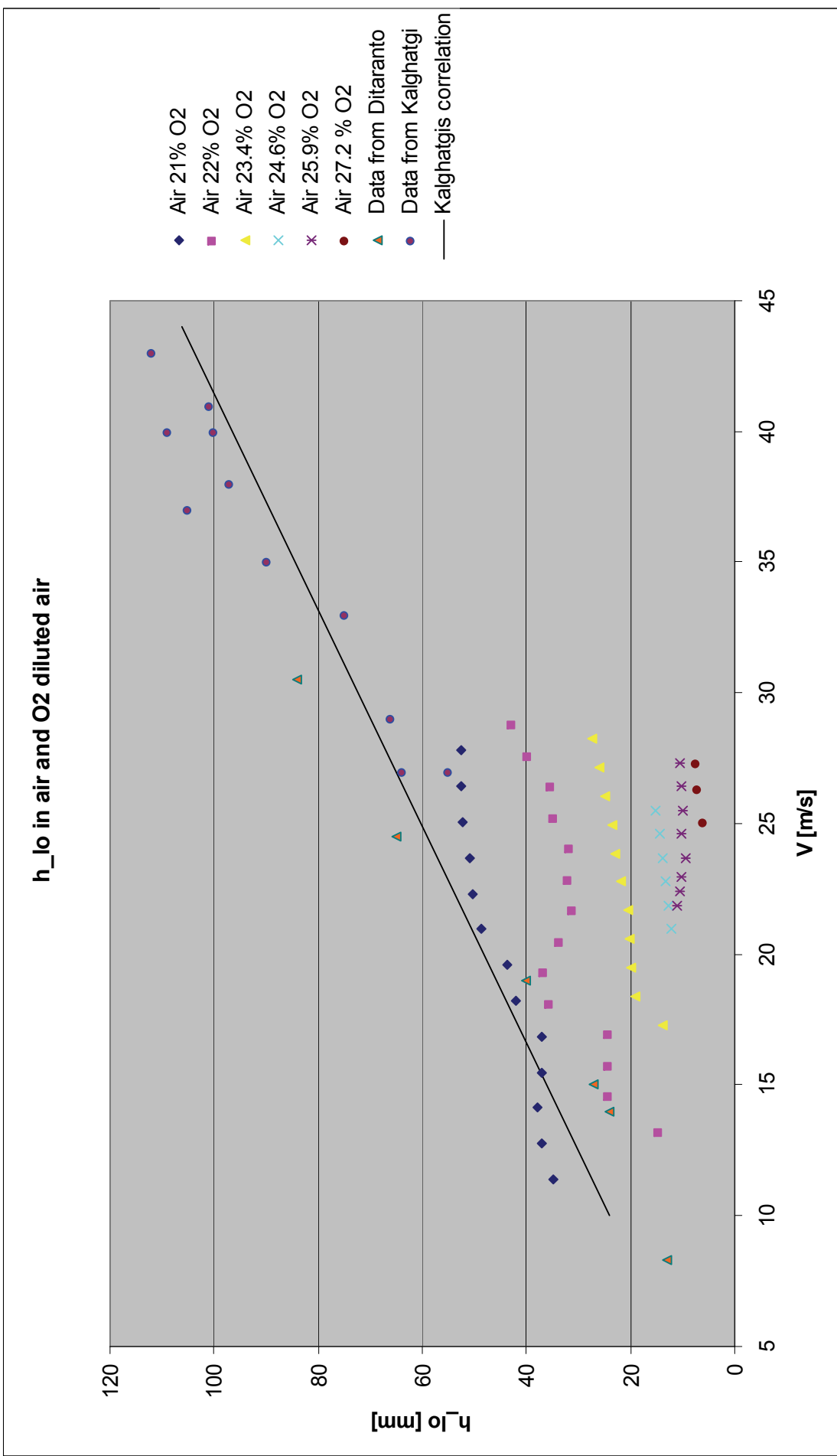
Figure 25 h_lo in air and oxygen enriched air with 5mm nozzle

The experiments on lift-off velocities were also carried out in air and oxygen enriched air and the results are presented in Figure 26. In good agreement with Kalghatgis conclusion that "The flame lift-off height varies linearly with jet exit velocity and is independent of burner diameter for a given gas" [16] it is seen that the lift-off velocity is independent of nozzle diameter. Blowout velocities are shown for the 2mm diameter nozzle only. The high velocities required could not be obtained with the larger nozzles because the increased mass flow rate caused depletion of oxygen in the combustion chamber.
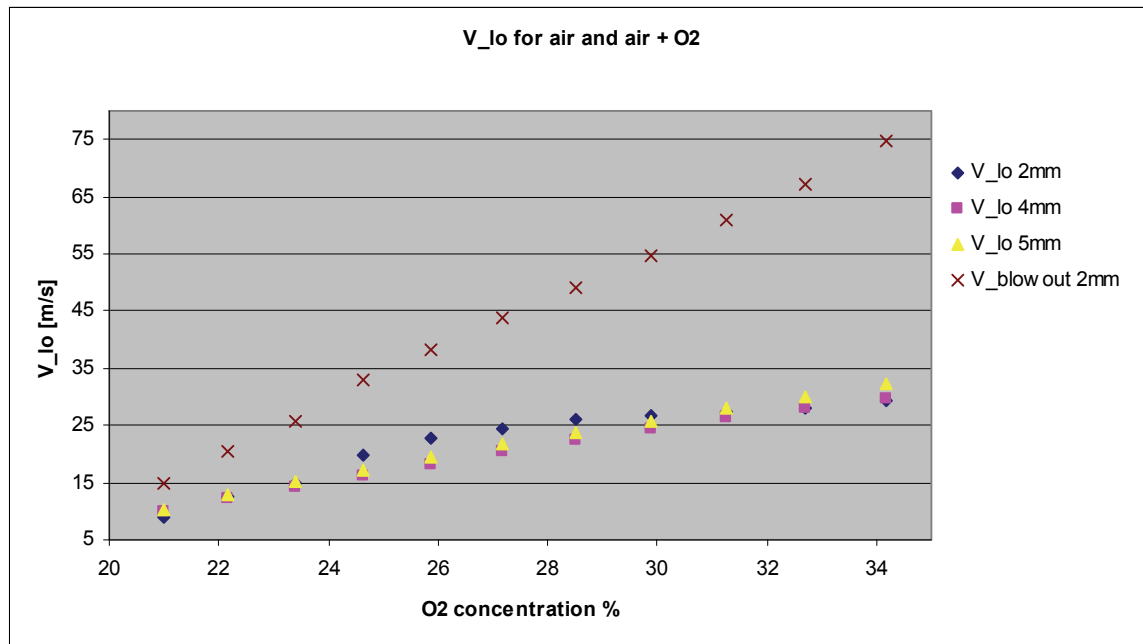

Figure 26 Lift-off velocities for air and oxygen enriched air

It is clear that higher oxygen concentration increases the lift-off velocity. Also, the interval in which a stable lifted flame is maintained increases with higher concentrations as one might expect.

4.1.1   Discussion of the effect of oxygen enriched air

As suspected, the flames in oxygen enriched environments have higher lift-off velocities and shorter lift-off heights with increasing oxygen concentration, and the slope of h_{lo} vs velocity is less steep for higher oxygen concentrations. This is most likely caused by the increased burning velocity caused by higher O_2 concentrations. There some irregularities in the results, especially for the 21% O_2 and 22% O_2 cases, which are puzzling and the measurements should perhaps be repeated for clarification.

The premixing theory assumes that lift-off heights depend on flame speed. Increased oxygen concentration means increased flame speed, so most of the experimental data are in good agreement with theory. Using Kalghatgis correlation (2.41) for lift-off height and changing the flame speed to values corresponding to that of the given oxygen concentration, we get the following graph (Figure 27) for a given fuel jet velocity of 25 m/s. (values of S_L from Bergs calculations for oxygen enriched combustion [25])
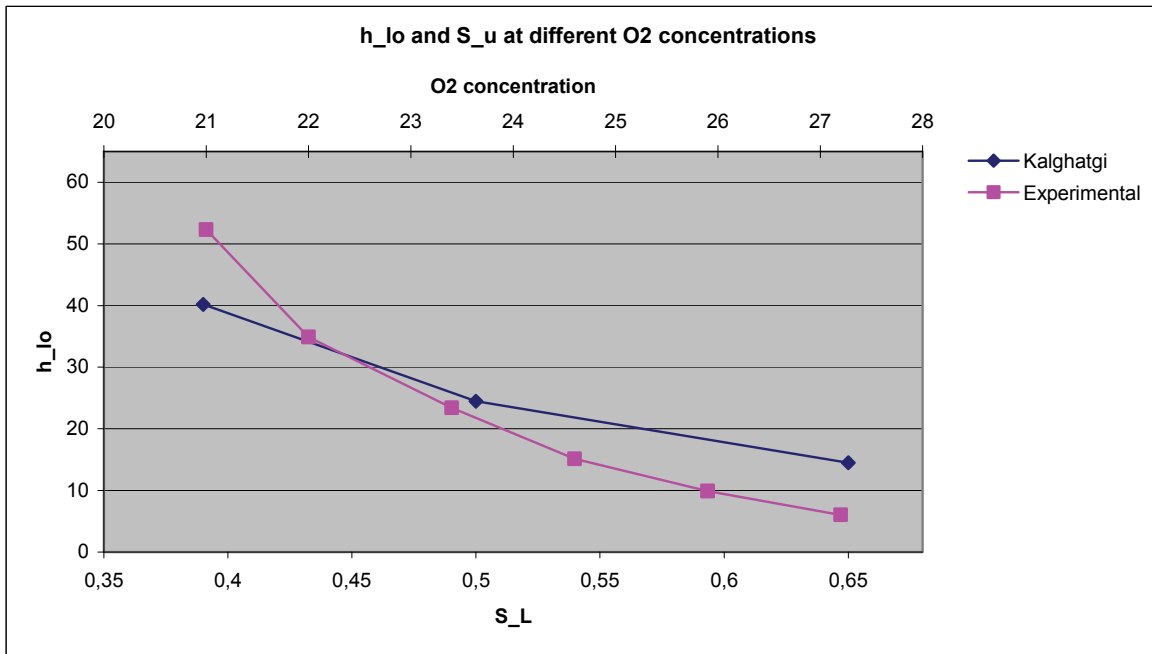
Figure 27 Lift-off heights and burning velocity for various oxygen concentrations at 25m/s jet velocity

The calculations are not in perfect agreement with the experimental results, however it gives a fair indication of h_{lo} and the trend is in correspondence with experimental results. An equivalence ratio of unity was assumed in the calculations, which could explain some of the irregularities. Also, eq. (2.41) does not take into account the effect of co-flow which could lead to higher h_{lo}, especially at lower oxygen concentrations. A third factor explaining the deviations could be that eq. (2.41) was developed with the use of various fuels, not alteration of oxidant to change S_L.

4.2 EFFECT OF HEAT RADIATION ON LIFT-OFF CHARACTERISTICS

Results from experiments on h_{lo} and V_{lo} for oxy-fuel flames were found to be influenced by the surrounding wall temperatures. It was observed that lift-off velocities were lower when the surrounding wall was at room temperature compared to the same flame with higher wall temperatures. Figure 28 shows an example of this effect. The wall temperature was measured at a height of 500 mm above the burner exit. The first case was done with an initial wall temperature of 89° C and it is seen that an increase in jet exit velocity yields little effect on h_{lo}. In the second case the initial wall temperature was 320° C, the effect of higher temperature is seen immediately as V_{lo} is increased from 18,2 m/s from the first case to 26.4 m/s in the second. Lift-off heights have also been significantly decreased in the second case. h_{lo} is 31,8 mm at 30, 9 m/s with cold wall, compared to h_{lo}=13,6 at 30 m/s for the cold wall. It is seen that there is no continuity between the two sets of results. Even though T_w is almost the same for case 1 at 26 m/s and case 2 at 34m/s, h_{lo} is very different. This indicates that the radiation effect alters the transition from attached to lifted flame. Besides, it should be noted that the T_w value is just an indication of wall radiation, it does not represent the whole radiation picture.
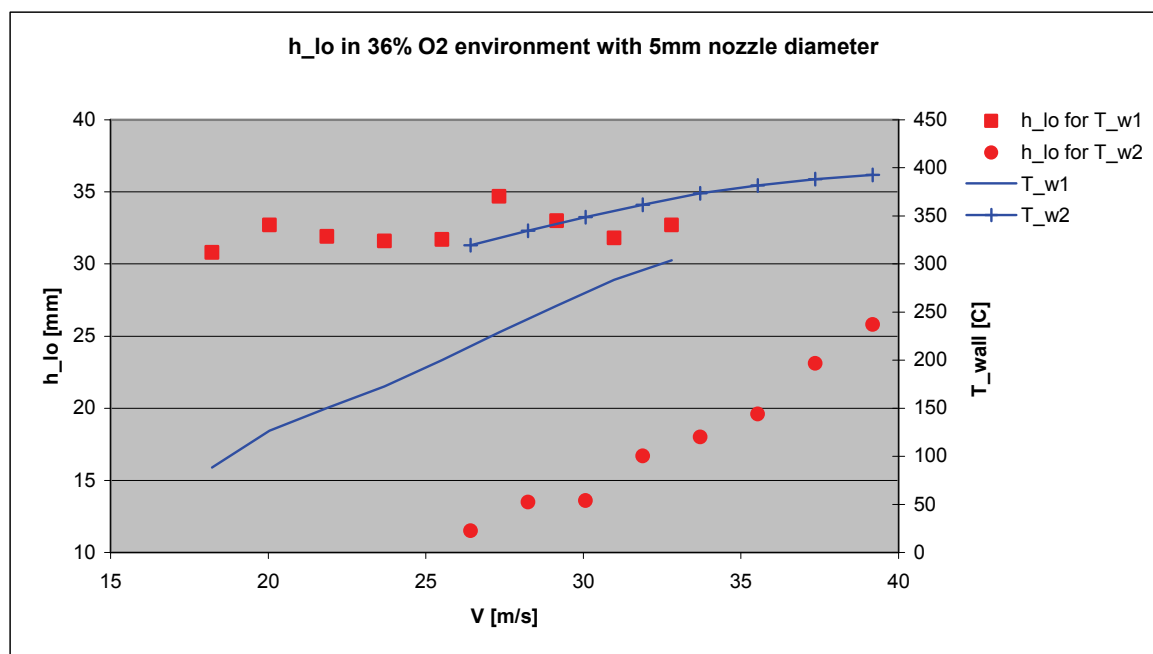

Figure 28 h_{lo} in 36% O_2 environment

Since the 5mm nozzle requires higher flow rates, hence higher heat release, than the 4mm and 2mm nozzle to get the same jet exit velocity, it proved difficult to get measurements for low wall temperatures using the 5mm nozzle.

The large flames heated the surrounding walls very fast, as shown in Figure 29. In less than nine minutes the temperature rises from 34° C and 53° C to 90° C and 216° C. At 500mm height the wall is heated up by convective heat transfer from the hot exhaust gases as well as the radiative heat transfer. This causes the wall temperature to increase faster at 500mm height than at 200mm where the gas temperature is much lower and heat transfer is mainly by radiation.
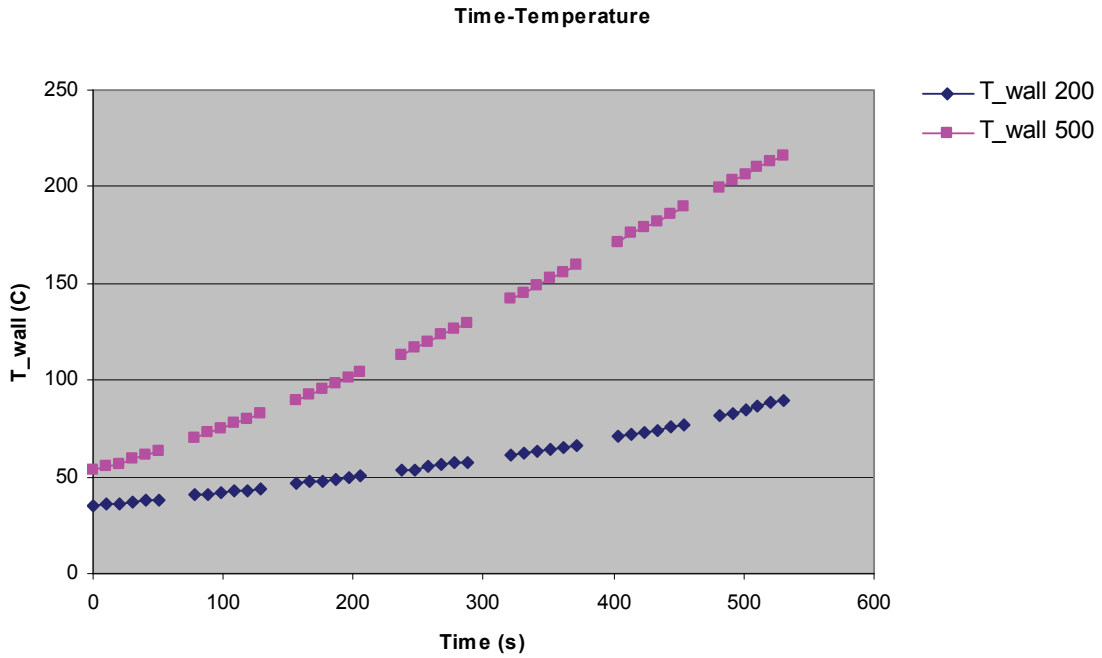
Time-Temperature

Figure 29 Wall temperature measurements in 34% O$_2$ with 5mm nozzle diameter.

In Figure 30 it can be seen that h$_{lo}$ actually *decreases* with increasing jet exit velocity, corresponding with increasing wall temperatures. This further indicates a dependency between lift-off characteristics and the surrounding wall temperatures.

Figure 30 h$_{lo}$ in 38% O$_2$ and 5mm nozzle diameter

To get measurements of h$_{lo}$ at low wall temperature, it was necessary to use larger steps between jet exit velocities to get data over a larger velocity span. An example of this is shown in Figure 31.

- 42 -

Figure 31 h$_{lo}$ in 34% O$_2$ with 5mm nozzle diameter

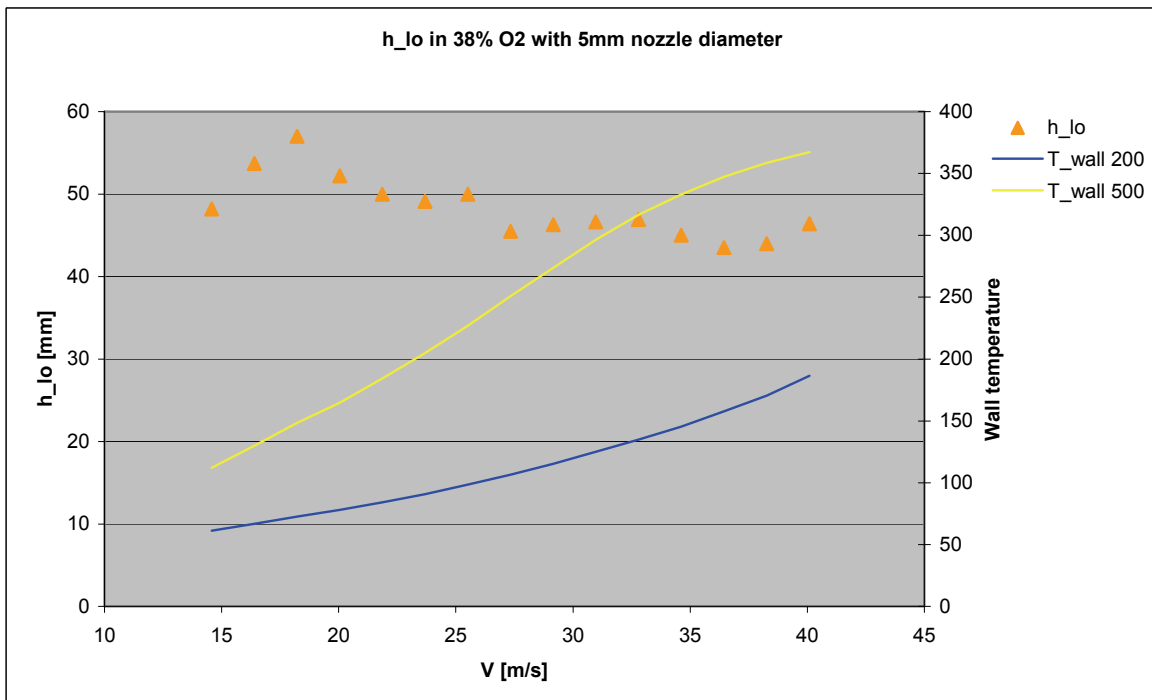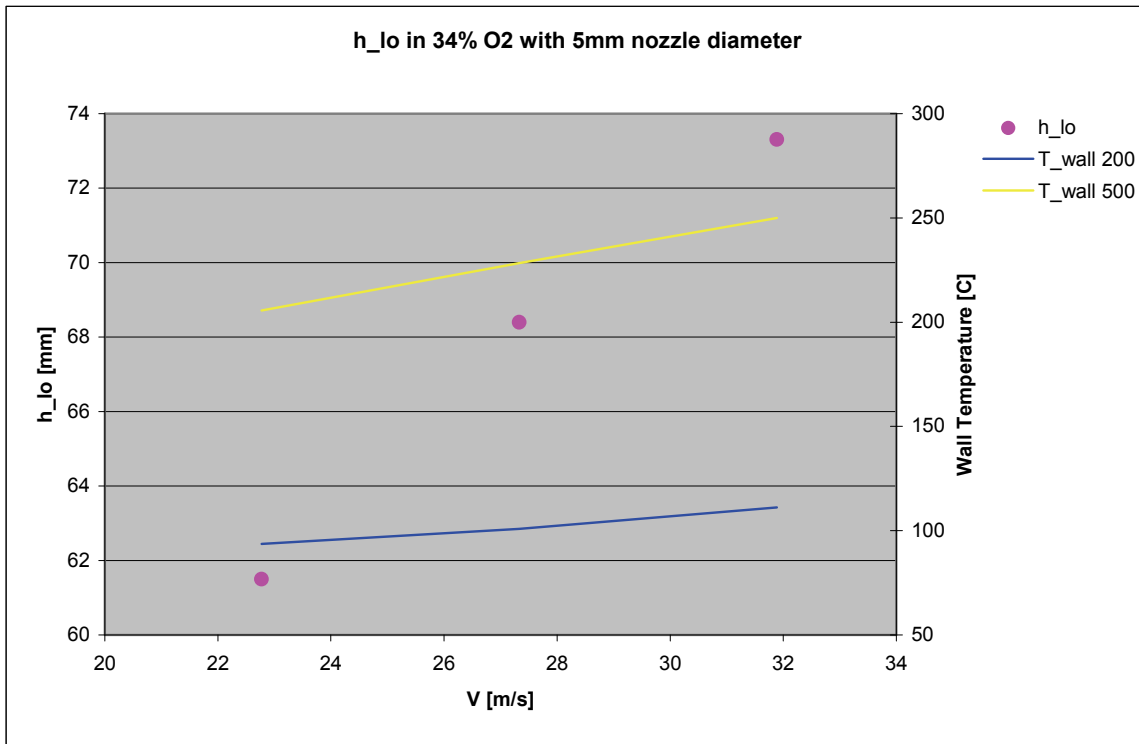### 4.2.1 Discussion of the effect of heat radiation

The high radiative and thermal capacity properties of CO_2 compared to nitrogen causes more efficient heat transfer from the flame. For this reason oxy-fuel flames below 30% O_2 concentration can not be stabilized due to the high heat transfer and low burning velocity [12]. Increasing the oxygen concentration causes higher burning velocities and a stable flame can be maintained. From the experiments it is observed that higher lift-off velocities and lower lift-off heights are closely related to oxygen concentration for flames in comparable surrounding temperatures.

As the surrounding wall temperature rises, the thermal loss from the flame will decrease substantially since thermal radiation is related to temperature by a power of four ($E = \sigma(T_f^4 - T_w^4)$) thereby further stabilizing the flame. The experimental results agree with this, as flames burning in the same environment seem to be more stabile at higher wall temperatures. Also, there seems to be a larger dependence on surrounding temperatures at lower oxygen concentrations, which may be caused by higher CO_2 concentrations. Several studies have indeed shown that when heat loss from the flame is reduced, S_L is increased [27, 28].

To get more accurate measurements, experiments should be conducted in a chamber were wall temperature can be controlled, perhaps by applying a coolant system. This way, precise measurements may be done at various wall temperatures.

4.3 EFFECT OF CO-FLOW GAS TEMPERATURE ON LIFT-OFF CHARACTERISTICS

The rather large pressure drop over the reduction valves on the gas containers caused the gas temperature to drop considerably. This was especially noticeable for CO_2 gas, where the reduction valve, mass flow controller and parts of the tubing would be covered in frost after a few minutes of operation.

When the pressure in the gas containers decreased, the pressure drop over the reduction valve decreased, and the gas temperature drop would be less severe. This caused the co-flow gas temperature to fluctuate and temperature measurements in the plenum ranged from around 7° C to about 20° C.

Figure 32 shows the lift-off height of two flames at different wall temperatures. Note that the flame with hot surroundings actually has lower V_{lo} and higher h_{lo} than the flame at colder surroundings.
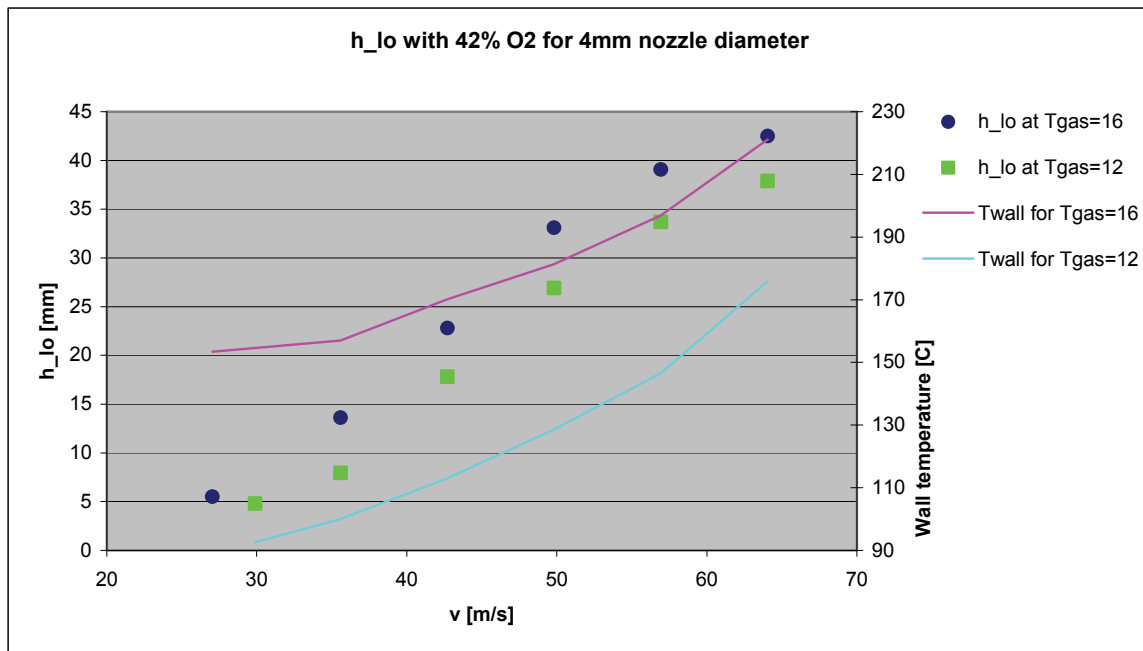
Figure 32 Gas temperature influence on h_lo

4.3.1 Discussion of the effect of co-flow gas temperature

It is difficult to make any conclusions surrounding the effect from co-flow temperature on combustion properties, since evidence were not consistent and there were difficulties separating the effect of wall temperature from the effects of co-flow temperature. However, the heat transfer properties of CO_2 are different from those of air, and it is a possibility that it could influence flame stability. In the future it would be advised to do experiments where the gas temperature could be controlled and varied, so that more precise measurement could be performed.

4.4 EFFECT OF O_2/CO_2 ENVIRONMENT ON LIFT-OFF CHARACTERISTICS

Figure 33 shows how the lift-off characteristics change with different oxidants. The results indicate that oxidants of O_2/CO_2 mixture require higher oxygen concentrations than oxidants of air and oxygen enriched air to achieve similar stability characteristics. As an example it can be seen that for the oxy-fuel case with 34% oxygen, only slightly lower lift-off heights are observed compared with the case of air with 23.4% oxygen.
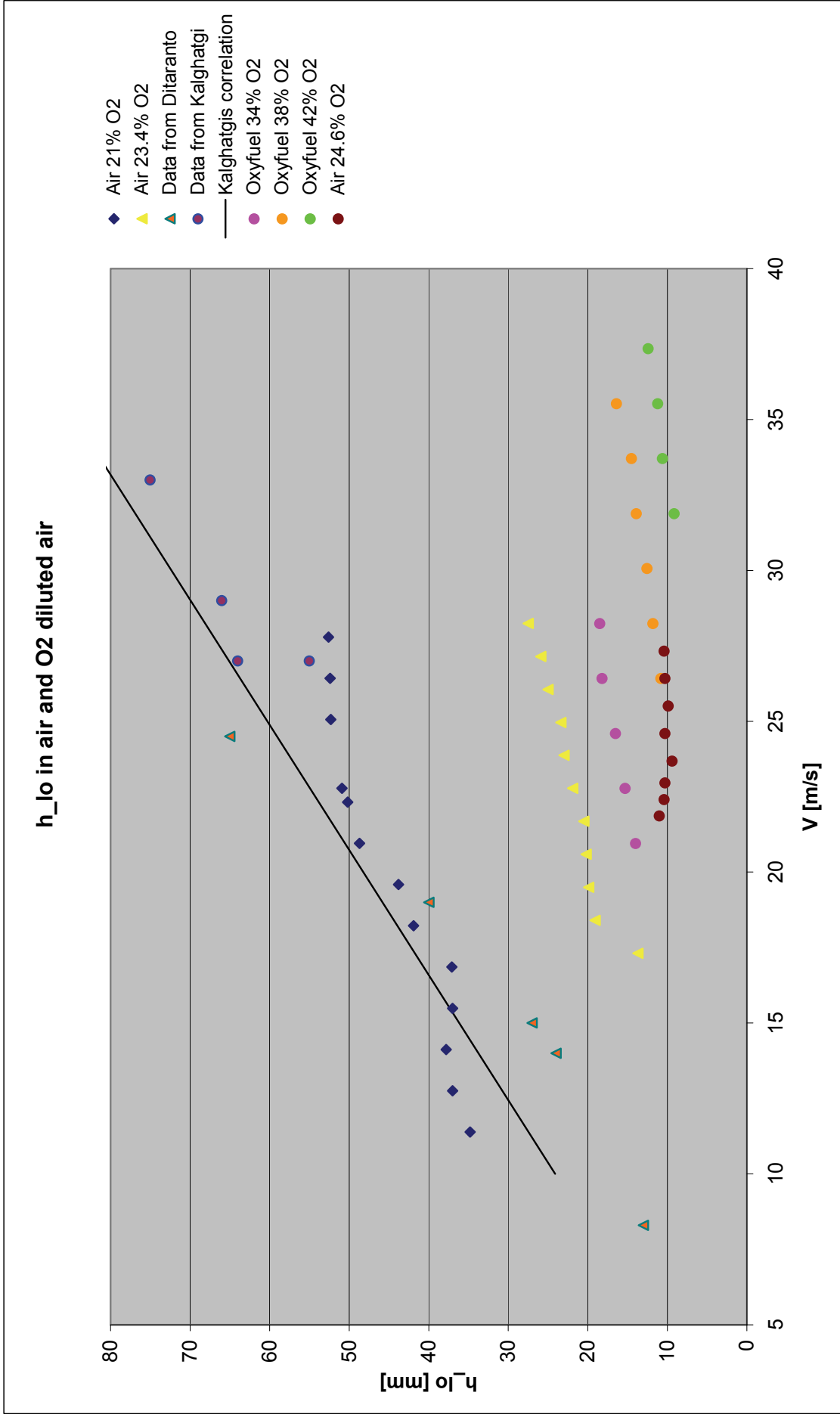
Figure 33 h_{lo} in various oxidants

Increasing the oxygen content in the O_2/CO_2 environment leads to higher burning velocities and hence higher lift-off velocities and lower lift-off heights. Results from all oxy-fuel experiments with 5mm nozzle are shown in Figure 34. Wall temperature for the first measurement on each flame is indicated in the legend as a reference. Sometimes measurements were stopped because of oxygen depletion, this is indicated with a (l) in the legend. If measurements were stopped because wall temperatures were too high, this is indicated by a (T) in the legend. For the occasions when measurements were stopped due to the lift-off height being outside the view of the camera, a (h) is used in the legend. A (b) in the legend indicates that measurements were stopped at the blowout velocity.

Measurements at the same oxygen concentration are the same color in the following graphs. For measurements done at low initial wall temperatures a triangle is used as symbol, a square indicates medium initial wall temperatures, and a warm wall is labeled with a circle.

The trend is very clear in that high oxygen concentrations and high temperatures give lower lift-off heights and higher lift-off velocities. In fact the trends show very little increase in h_{lo} because of the trade-off between higher S_L and lower heat loss. However, the effect of surrounding wall temperature results in some measurements being highly irregular.

Results from measurements with 4mm nozzle diameter are shown in Figure 35. Since the mass flow rate is lower with than with the 5mm pipe, the wall temperature increase is slower, thus making it easier to do measurements. Also, higher jet velocities are accessible without oxygen depletion.

Figure 36 displays the results from the 2mm diameter nozzle. Using this nozzle it was not possible to get a stable lifted flame at oxygen concentrations below 38%, this could be caused the co-flow velocity or it could be that the mass flow controller had difficulties maintaining a stable flow at these very low volumetric flow rates (below 5% of maximum flow). The low flow rates also meant lower flame power, and the wall temperature increase was less severe than in both the 5mm and 4mm case.

In Figure 37 the dimensionless lift-off height $\dfrac{h_{lo}}{d}$ is plotted for velocity to compare the different nozzles. It can be observed that the slope for the 2mm and 4mm nozzle flames are comparable, but the slopes of the 5mm nozzle flames are less steep.

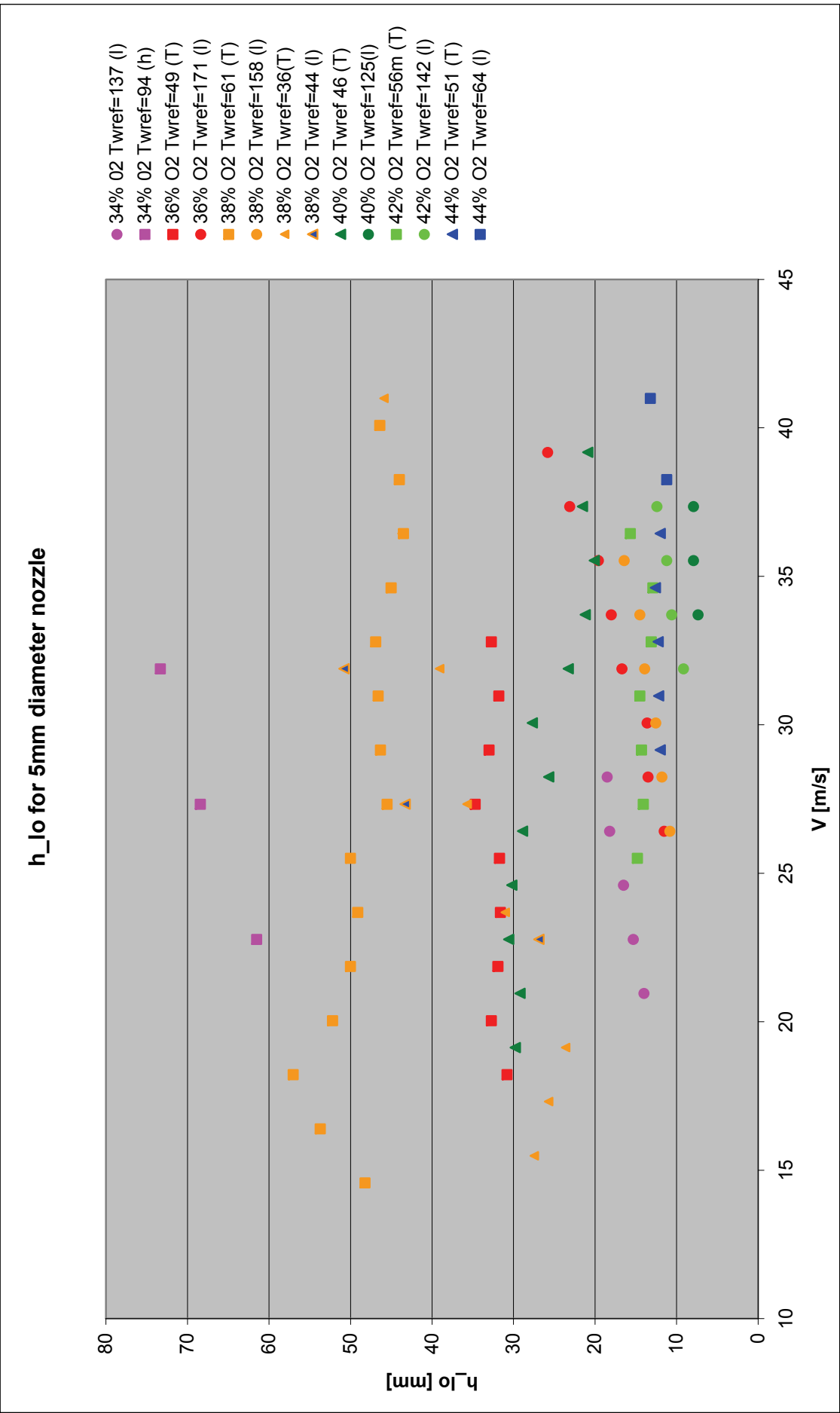**Figure 34 h_lo for different oxygen concentrations for the 5mmozzle**
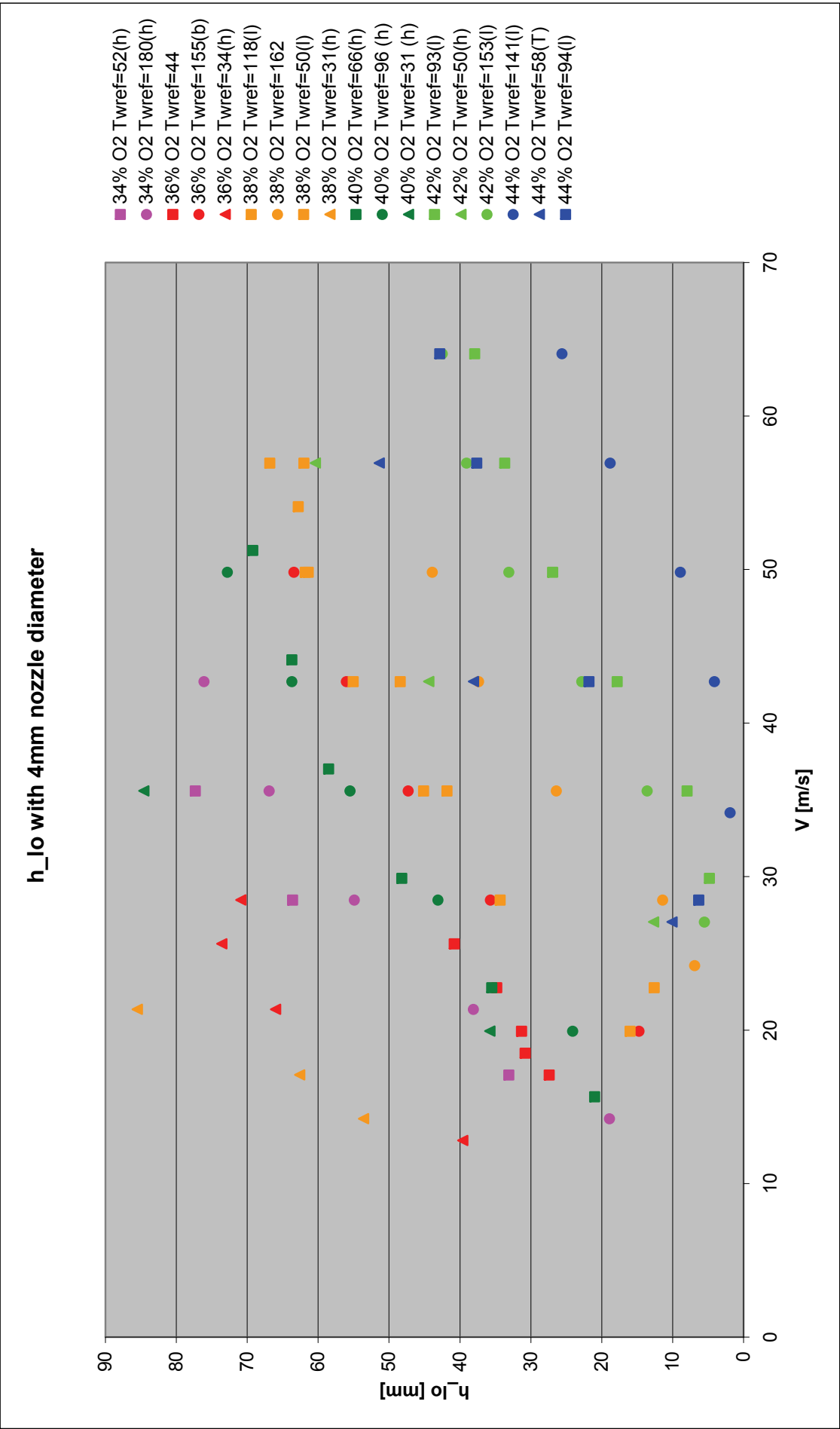
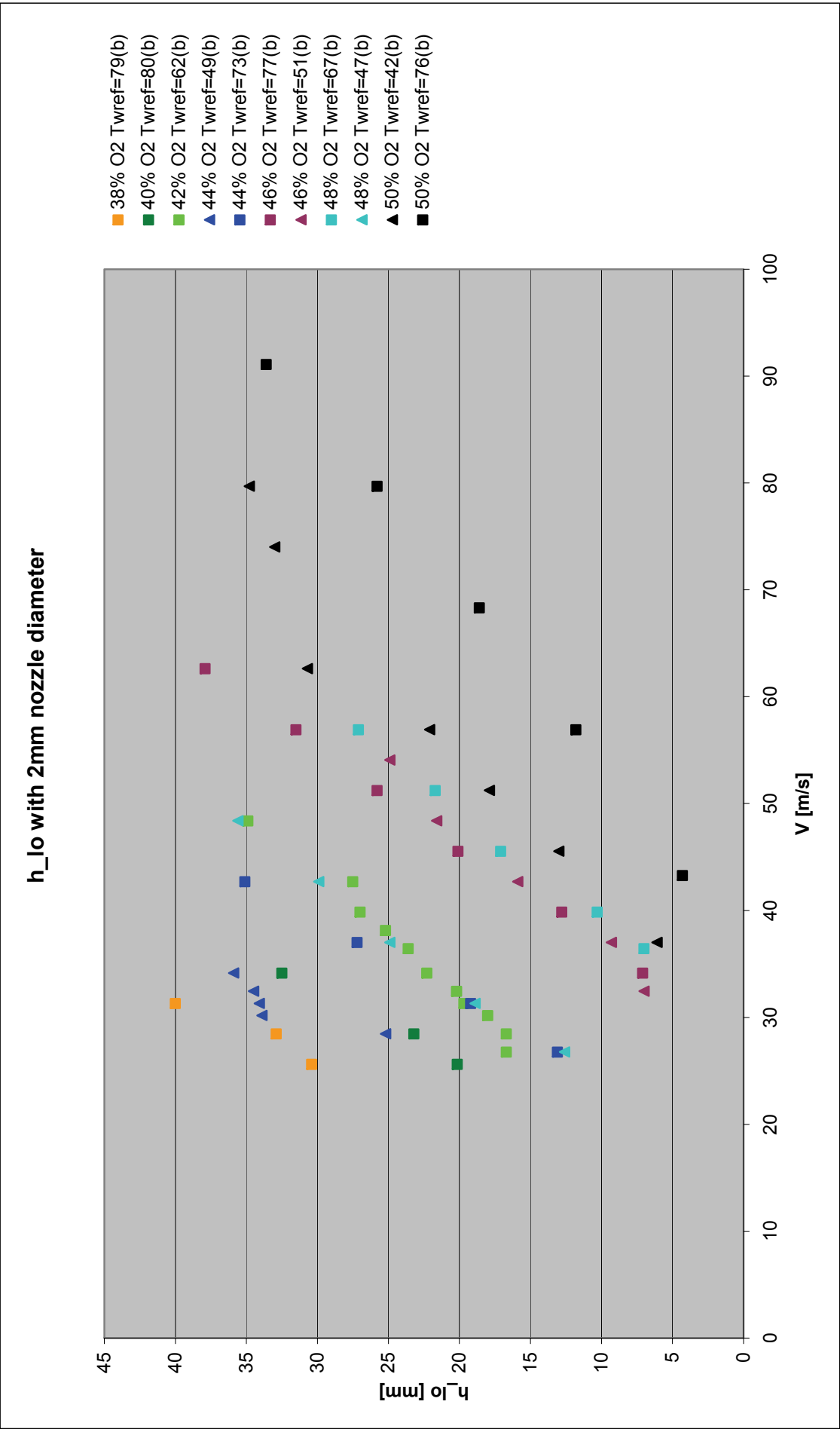**Figure 35 hlo measurements with 4mm nozzle diameter**

Figure 36 hlo measurements with 4mm nozzle diameter
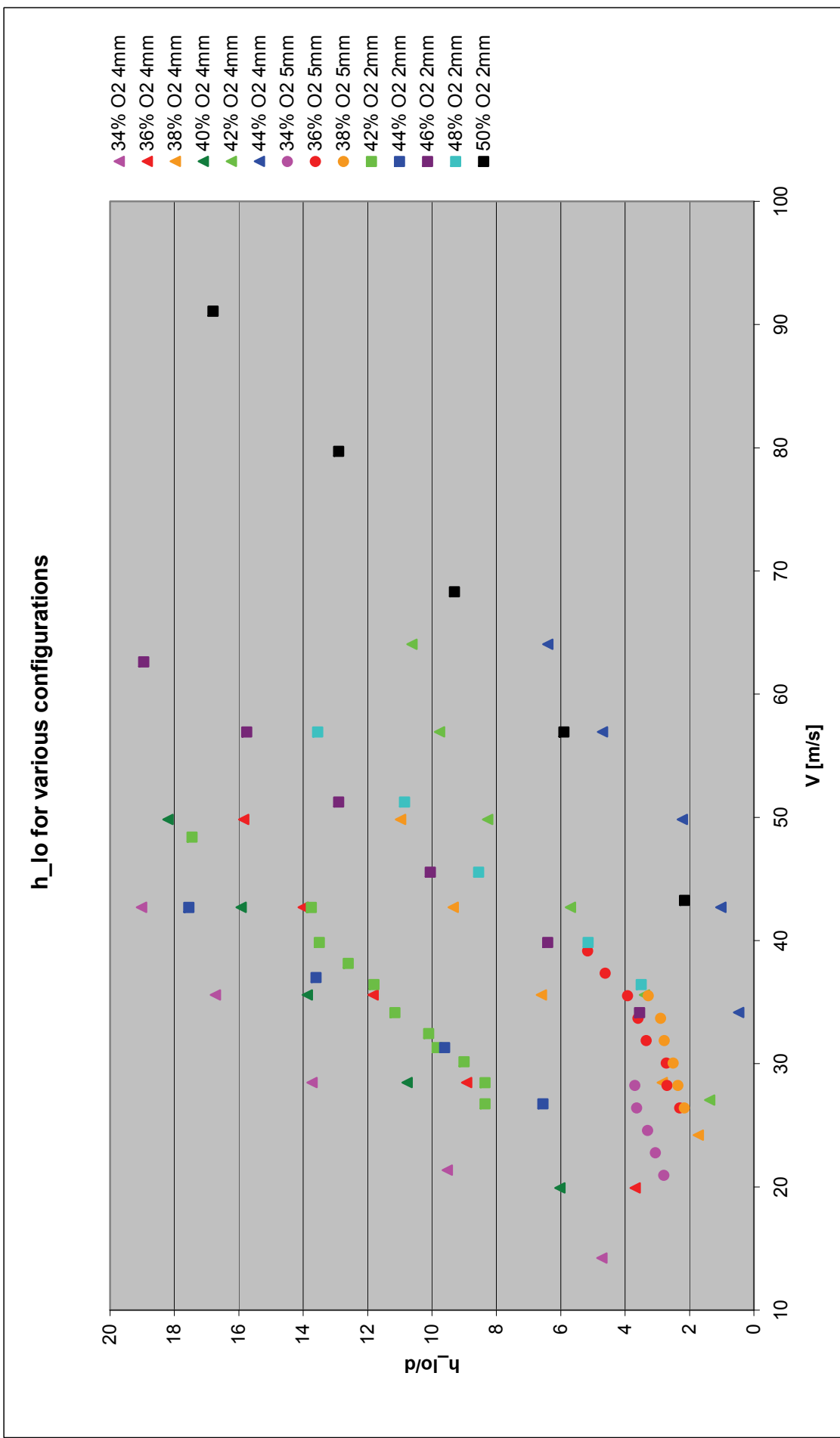
Figure 37 h_lo/d for selected flames, plotted for Reynolds number

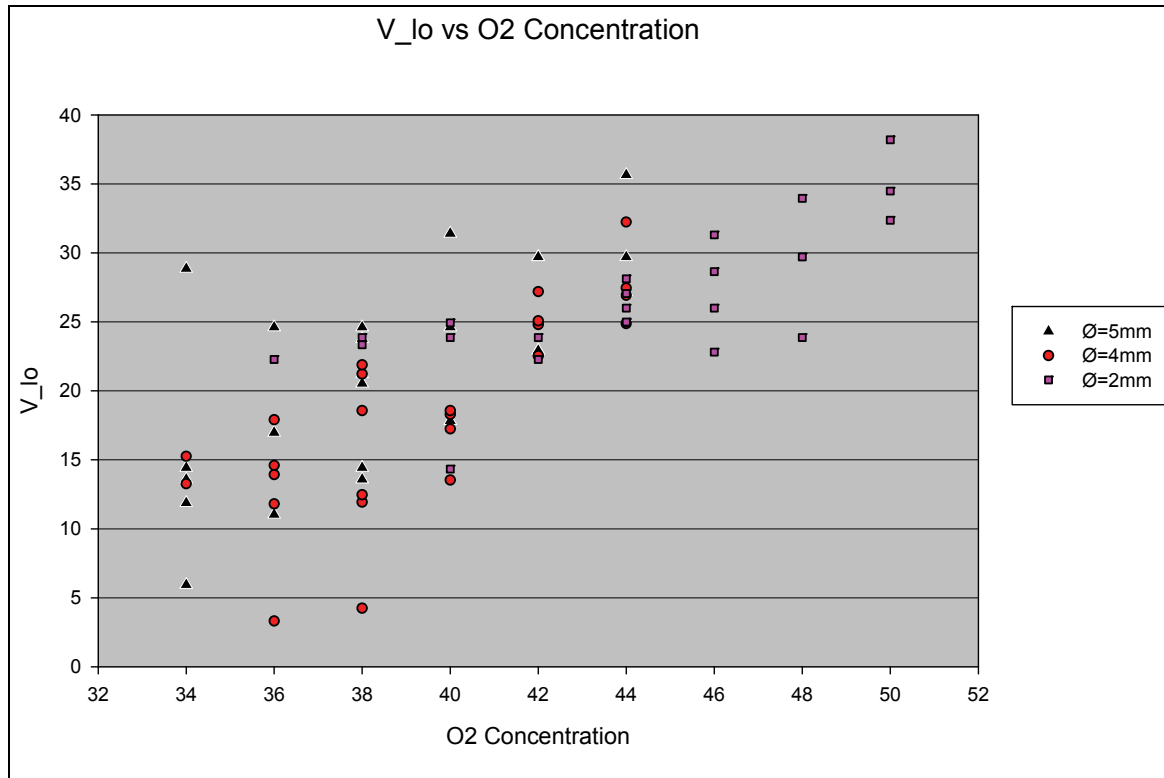Figure 38 shows how V_{lo} is affected by oxygen concentration.

Figure 38 V_{lo} for various oxygen concentrations and nozzle diameters.

For the 2mm diameter nozzle the flame would blowout directly at lower concentrations than 36% oxygen. Above 44% O_2 concentration the mass flow rates needed to reach lift-off velocities with the 4mm and 5mm nozzles resulted in oxygen depletion. Thus, V_{lo} values above 44% O_2 concentrations were only found for the 2mm nozzle.

Variations in V_{lo} are greater at low O_2 concentrations, indicating a greater dependency on the surrounding temperature for flames in high CO_2 concentration environments.

The flame fluctuations were measured by finding the height of 75% intensity (h_{75}) and 25% intensity (h_{25}) from the normalized pictures, and the fluctuations were defined as $h_{75} - h_{25} = \Delta h$ (see section 3.2). A few examples are shown in Figure 39, lift-off heights and fluctuations are plotted for Reynolds number. Fluctuations are marked with dh in the legend.

It is seen that higher velocities and higher Reynolds number are associated with larger fluctuations in the flame. Also, the fluctuations are larger for lower oxygen concentrations and higher lift-off heights. This again indicates that higher oxygen concentrations cause the flame to be more stable.
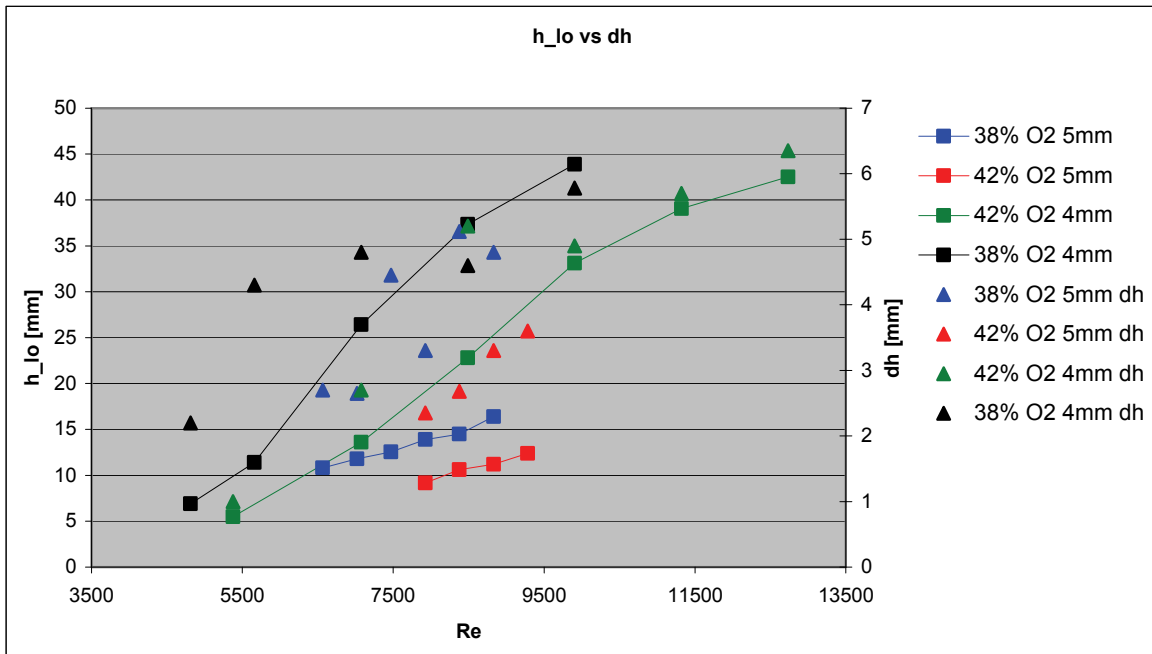
Figure 39 Lift-off heights and fluctuations for Reynolds number

A comparison of experimental values and Kalghatgis correlation (2.41) is shown in Figure 40. Flame speeds were taken from Ditarantos calculations (fig.2).
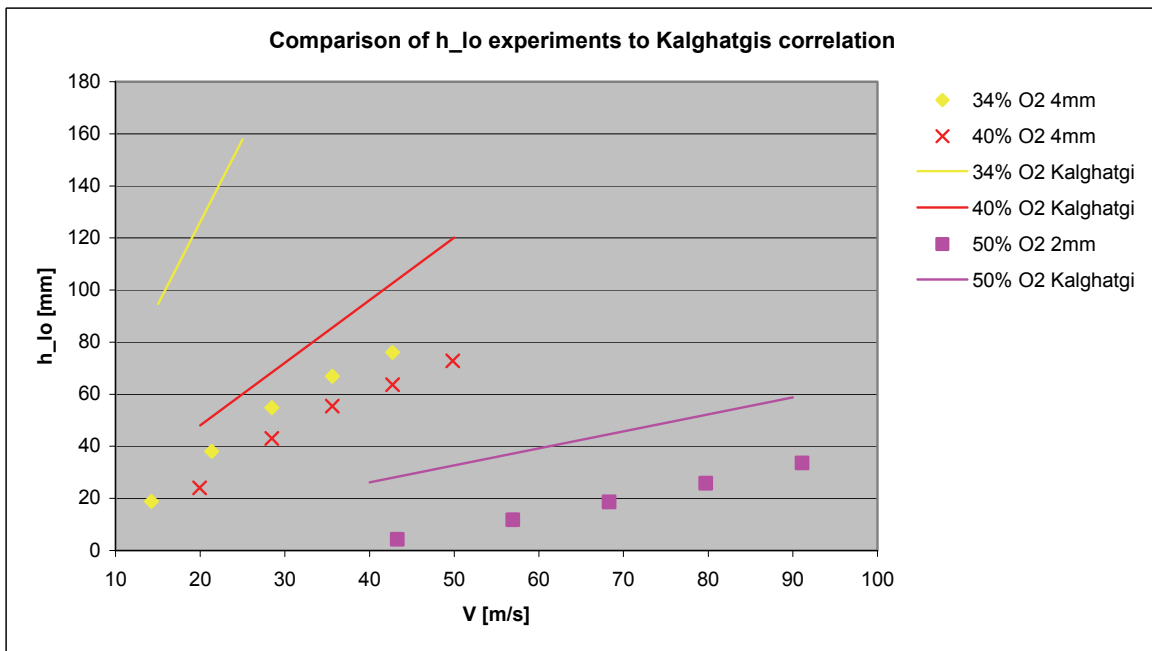

Figure 40 Comaparing Kalghatgis correlation and experimental data

4.4.1 Discussion of the effect of O_2/CO_2 environment

The overall trend is that in O_2/CO_2 environments, higher oxygen concentrations result in lower lift-off heights and more stable flames since increasing O_2 concentrations cause higher flame speeds. However, the effects of wall temperature and perhaps also gas temperature cause the stability behavior to be modified. If for example experiments in 40% O2 environment are to be performed, ideally two or three measurements should be done, but the changes in surrounding walls would cause very different results.

The most concise measurements came from using the 2mm nozzle, because with low flame power longer time is needed to heat the wall. On the other hand the 5mm nozzle gave very challenging experiments because of high flame powers and quickly rising wall temperatures.

Kalghatgis correlation was compared with experimental measurements but showed rather large deviations on lift-off height. This could be caused by the equation not taking into account the effect of heat loss. The rate of change in h_{lo} to jet velocity fits fairly well though, particularly for higher O_2 concentrations.

5   CONCLUSIONS

Experimental measurements on lift-off heights and velocities for oxy-fuel combustion were conducted in SINTEFs rig for diffusion flames. The measurements were done in oxygen concentrations ranging from 34% to 50% , and with nozzle diameters of 2mm, 4mm and 5mm. As a reference, measurements using air, and oxygen enriched air, as oxidant, were performed, and were shown to correspond well with earlier measurements.

The experiments showed that increasing oxygen concentration leads to higher lift-off velocities and lower lift-off heights, most likely due to increasing flame speed for higher O_2 concentrations. It was observed that flame stability and lift-off characteristics were very irregular for oxy-fuel combustion, with lift-off heights ranging from 15mm to 61mm for the same flame configurations. The most probable explanation for this behavior was found to be heat radiation to the surroundings affecting burning velocity.

Since these irregularities were not found in any of the cases where air and oxygen enriched air was used as oxidant, it is likely that the presence of CO_2 is important in this regard. Unlike nitrogen, CO_2 absorbs and emits heat radiation. It is thought that this could have a quenching effect on the flame when the surroundings are cold. This theory is further supported by the observation of larger irregularities for higher CO_2 concentrations.

In a few experiments it could be argued that the co-flow gas temperature had an effect on flame stabilization. However, too few observations of this behavior were made to draw any conclusions.

5.1   PROPOSALS FOR FUTURE WORK

More experiments should be carried out to get better and more consistent data on the effect of heat radiation on oxy-fuel combustion. A new combustion chamber is already planned for such measurements, with a built in system of water cooling to control wall temperatures. This will allow more precise measurements, and should provide interesting results.

To get better measurements with regards to the proposed effect of co-flow gas temperature on lift-off stability, proper control of gas temperature should be integrated in the rig.

Time constraints and challenging measurements meant that the experiments on hysteresis behavior in oxy-fuel flames were not conducted. A comparison of hysteresis in oxy-fuel and in air would be interesting, and could be performed in the new rig as well.

Also, experimental measurements in air, and oxygen enriched air, should be carried out again to perhaps get better results than those presented here. Especially the measurements in air with 21% and 22% oxygen show behavior that cannot be explained properly.

6 REFERENCES

1.   Bolland, O. and H. Undrum, *A novel methodology for comparing CO2 capture options for natural gas-fired combined cycle plants.* Advances in Environmental Research, 2003. **7**(4): p. 901-911.

2.   Lyons, K.M., *Toward an understanding of the stabilization mechanisms of lifted turbulent jet flames: Experiments.* Progress in Energy and Combustion Science, 2007. **33**(2): p. 211-231.

3.   Pitts, W.M., *Assessment of theories for the behavior and blowout of lifted turbulent jet diffusion flames.* Symposium (International) on Combustion, 1989. **22**(1): p. 809-816.

4.   Turns, S.R., *An introduction to combustion : concepts and applications*. 2nd ed. McGraw-Hill series in mechanical engineering. 2000, Boston: WCB/McGraw-Hill. xxiii, 676 p.

5.   White, F.M., *Viscous fluid flow*. 3. ed. McGraw-Hill international edition. 2006, Boston [u.a.]: McGraw-Hill. XXI, 629 S.

6.   Warnatz, J., U. Maas, and R.W. Dibble, *Combustion : physical and chemical fundamentals, modeling and simulation, experiments, pollutant formation*. 3rd ed. 2001, Berlin ; New York: Springer. x, 299 p.

7.   Incropera, F.P., *Fundamentals of heat and mass transfer*. 6th ed. 2007, Hoboken, NJ: John Wiley. xxv, 997 p.

8.   Ludwig, C.B. and George C. Marshall Space Flight Center., *Handbook of infrared radiation from combustion gases*. Nasa Sp-3080. 1973, Washington,: Scientific and Technical Information Office, National Aeronautics and Space Administration; [for sale by the National Technical Information Service, Springfield. xi, 486 p.

9.   Hottel, H.C., *Radiant-Heat Transmission*, in *Heat Transmission*. 1954, McGraw-Hill: New York.

10.   Zizak, G., *Flame Emission Spectroscopy: Fundamentals and Applications.*, in *ICS Training Course on Laser Diagnostics of Combustion Processes*. 2000: University of Cairo, Egypt.

11.   De Leo, M., et al., *OH and CH luminescence in opposed flow methane oxy-flames.* Combustion and Flame, 2007. **149**(4): p. 435-447.

12.   Ditaranto, M. and J. Hals, *Combustion instabilities in sudden expansion oxy-fuel flames.* Combustion and Flame, 2006. **146**(3): p. 493-512.

13.   Oppelt, T., Ditaranto M., *Experimental study on Radiative Heat Flux From Oxy-Fuel Flames*. 2008, SINTEF Energy Research. p. 49.

14.   Buhre, B.J.P., et al., *Oxy-fuel combustion technology for coal-fired power generation.* Progress in Energy and Combustion Science, 2005. **31**(4): p. 283-307.

15.   Buckmaster, J., *Edge-flames.* Progress in Energy and Combustion Science, 2002. **28**(5): p. 435-475.

16.   Gautam, T., *Lift-off Heights and Visible Lengths of Vertical Turbulent Jet Diffusion Flames in Still Air.* Combustion Science and Technology, 1984. **41**(1): p. 17 - 29.

17.   Iyogun, C.O. and M. Birouk, *Effect of Fuel Nozzle Geometry on the Stability of a Turbulent Jet Methane Flame.* Combustion Science and Technology, 2008. **180**(12): p. 2186-2209.

18.   Leung, T. and I. Wierzba, *The effect of co-flow stream velocity on turbulent non-premixed jet flame stability.* Proceedings of the Combustion Institute, 2009. **32**: p. 1671-1678.

19.   Vanquick.L and Vantigge.A, *Stabilization Mechanism of Lifted Diffusion Flames.* Combustion and Flame, 1966. **10**(1): p. 59-&.

20.   Peters, N. and F.A. Williams, *Liftoff Characteristics of Turbulent Jet Diffusion Flames.* Aiaa Journal, 1983. **21**(3): p. 423-429.

21.   Joedicke, A., N. Peters, and M. Mansour, *The stabilization mechanism and structure of turbulent hydrocarbon lifted flames.* Proceedings of the Combustion Institute, 2005. **30**: p. 901-909.

22.   Broadwell, J.E., W.J.A. Dahm, and M.G. Mungal, *Blowout of turbulent diffusion flames.* Symposium (International) on Combustion, 1985. **20**(1): p. 303-310.

23.   Miake-Lye, R.C. and J.A. Hammer, *Lifted turbulent jet flames: A stability criterion based on the jet large-scale structure.* Symposium (International) on Combustion, 1989. **22**(1): p. 817-824.

24.   Weiland, N.T. and P.A. Strakey, *Stability Characteristics of Turbulent Hydrogen Dilute Diffusion Flames.* Combustion Science and Technology, 2009. **181**(5): p. 756-781.

25.   Berg, H., *Oxygen Enriched Combustion*. 1997, NTNU: Trondheim.

26.   Ditaranto, M., M. Fossum, and J.E. Hustad, *STABILITY AND DYNAMIC DEVELOPMENT OF METHANE-ENRICHED LOW CALORIFIC VALUE GAS FLAMES.* 2004. **5**(1): p. 16.

27.   Ju, Y., G. Masuya, and P.D. Ronney, *Effects of radiative emission and absorption on the propagation and extinction of premixed gas flames.* Symposium (International) on Combustion, 1998. **27**(2): p. 2619-2626.

28.   Chen, Z., et al., *Studies of radiation absorption on flame speed and flammability limit of CO2 diluted methane flames at elevated pressures.* Proceedings of the Combustion Institute, 2007. **31**: p. 2693-2700.